



Westinghouse
Electric Corporation

Energy Systems

Box 355
Pittsburgh Pennsylvania 15230-0355

AW-96-919

January 29, 1996

Document Control Desk
U.S. Nuclear Regulatory Commission
Washington, D.C. 20555

ATTENTION: MR. T. R. QUAY

APPLICATION FOR WITHHOLDING PROPRIETARY
INFORMATION FROM PUBLIC DISCLOSURE

SUBJECT: WESTINGHOUSE RESPONSES TO NRC REQUESTS FOR ADDITIONAL
INFORMATION ON THE AP600

Dear Mr. Quay:

The application for withholding is submitted by Westinghouse Electric Corporation ("Westinghouse") pursuant to the provisions of paragraph (b)(1) of Section 2.790 of the Commission's regulations. It contains commercial strategic information proprietary to Westinghouse and customarily held in confidence.

The proprietary material for which withholding is being requested is identified in the proprietary version of the subject report. In conformance with 10CFR Section 2.790, Affidavit AW-96-919 accompanies this application for withholding setting forth the basis on which the identified proprietary information may be withheld from public disclosure.

Accordingly, it is respectfully requested that the subject information which is proprietary to Westinghouse be withheld from public disclosure in accordance with 10CFR Section 2.790 of the Commission's regulations.

Correspondence with respect to this application for withholding or the accompanying affidavit should reference AW-96-919 and should be addressed to the undersigned.

Very truly yours,

Brian A. McIntyre, Manager
Advanced Plant Safety and Licensing

/nja

cc: Kevin Bohrer NRC 12H5

9602020088 960129
PDR ADOCK 05200003
A PDR

ATTACHMENT A

NTD-NRC-96-4632

RAI's addressed in the January 29, 1996 submittal:

| | |
|----------|---------|
| LOFTRAN: | 440.280 |
| | 440.285 |
| | 440.290 |
| | 440.302 |
| | 440.314 |
| | 440.460 |

| | |
|---------|---------|
| NOTRUMP | 440.542 |
| | 440.547 |
| | 440.553 |

| | |
|--------|---------|
| SPES-2 | 480.242 |
|--------|---------|

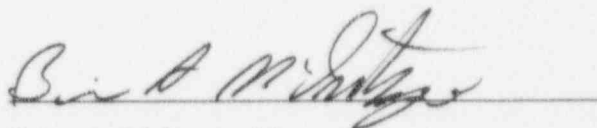
AFFIDAVIT

COMMONWEALTH OF PENNSYLVANIA:

ss

COUNTY OF ALLEGHENY:

Before me, the undersigned authority, personally appeared Brian A. McIntyre, who, being by me duly sworn according to law, deposes and says that he is authorized to execute this Affidavit on behalf of Westinghouse Electric Corporation ("Westinghouse") and that the averments of fact set forth in this Affidavit are true and correct to the best of his knowledge, information, and belief:



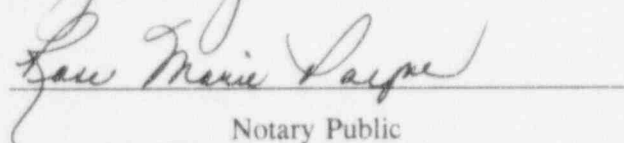
Brian A. McIntyre, Manager

Advanced Plant Safety and Licensing

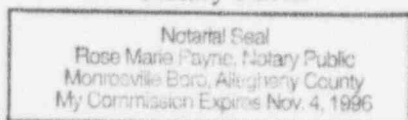
Sworn to and subscribed

before me this 29 day

of January, 1996



Notary Public



2661A

Member, Pennsylvania Association of Notaries

- (1) I am Manager, Advanced Plant Safety And Licensing, in the Advanced Technology Business Area, of the Westinghouse Electric Corporation and as such, I have been specifically delegated the function of reviewing the proprietary information sought to be withheld from public disclosure in connection with nuclear power plant licensing and rulemaking proceedings, and am authorized to apply for its withholding on behalf of the Westinghouse Energy Systems Business Unit.
- (2) I am making this Affidavit in conformance with the provisions of 10 C.F.R. Section 2.790 of the Commission's regulations and in conjunction with the Westinghouse application for withholding accompanying this Affidavit.
- (3) I have personal knowledge of the criteria and procedures utilized by the Westinghouse Energy Systems Business Unit in designating information as a trade secret, privileged or as confidential commercial or financial information.
- (4) Pursuant to the provisions of paragraph (b)(4) of Section 2.790 of the Commission's regulations, the following is furnished for consideration by the Commission in determining whether the information sought to be withheld from public disclosure should be withheld.
 - (i) The information sought to be withheld from public disclosure is owned and has been held in confidence by Westinghouse.
 - (ii) The information is of a type customarily held in confidence by Westinghouse and not customarily disclosed to the public. Westinghouse has a rational basis for determining the types of information customarily held in confidence by it and, in that connection, utilizes a system to determine when and whether to hold certain types of information in confidence. The application of that system and the substance of that system constitutes Westinghouse policy and provides the rational basis required.

Under that system, information is held in confidence if it falls in one or more of several types, the release of which might result in the loss of an existing or potential competitive advantage, as follows:

- (a) The information reveals the distinguishing aspects of a process (or component, structure, tool, method, etc.) where prevention of its use by any of Westinghouse's competitors without license from Westinghouse constitutes a competitive economic advantage over other companies.
- (b) It consists of supporting data, including test data, relative to a process (or component, structure, tool, method, etc.), the application of which data secures a competitive economic advantage, e.g., by optimization or improved marketability.
- (c) Its use by a competitor would reduce his expenditure of resources or improve his competitive position in the design, manufacture, shipment, installation, assurance of quality, or licensing a similar product.
- (d) It reveals cost or price information, production capacities, budget levels, or commercial strategies of Westinghouse, its customers or suppliers.
- (e) It reveals aspects of past, present, or future Westinghouse or customer funded development plans and programs of potential commercial value to Westinghouse.
- (f) It contains patentable ideas, for which patent protection may be desirable.

There are sound policy reasons behind the Westinghouse system which include the following:

- (a) The use of such information by Westinghouse gives Westinghouse a competitive advantage over its competitors. It is, therefore, withheld from disclosure to protect the Westinghouse competitive position.
- (b) It is information which is marketable in many ways. The extent to which such information is available to competitors diminishes the Westinghouse ability to sell products and services involving the use of the information.

- (c) Use by our competitor would put Westinghouse at a competitive disadvantage by reducing his expenditure of resources at our expense.
 - (d) Each component of proprietary information pertinent to a particular competitive advantage is potentially as valuable as the total competitive advantage. If competitors acquire components of proprietary information, any one component may be the key to the entire puzzle, thereby depriving Westinghouse of a competitive advantage.
 - (e) Unrestricted disclosure would jeopardize the position of prominence of Westinghouse in the world market, and thereby give a market advantage to the competition of those countries.
 - (f) The Westinghouse capacity to invest corporate assets in research and development depends upon the success in obtaining and maintaining a competitive advantage.
- (iii) The information is being transmitted to the Commission in confidence and, under the provisions of 10CFR Section 2.790, it is to be received in confidence by the Commission.
- (iv) The information sought to be protected is not available in public sources or available information has not been previously employed in the same original manner or method to the best of our knowledge and belief.
- (v) Enclosed is Letter NTD-NRC-96-4632, January 29, 1996 being transmitted by Westinghouse Electric Corporation (W) letter and Application for Withholding Proprietary Information from Public Disclosure, Brian A. McIntyre (W), to Mr. T. R. Quay, Office of NRR. The proprietary information as submitted for use by Westinghouse Electric Corporation is in response to questions concerning the AP600 plant and the associated design certification application and is expected to be applicable in other licensee submittals in response to certain NRC requirements for justification of licensing advanced nuclear power plant designs.

This information is part of that which will enable Westinghouse to:

- (a) Demonstrate the design and safety of the AP600 Passive Safety Systems.
- (b) Establish applicable verification testing methods.
- (c) Design Advanced Nuclear Power Plants that meet NRC requirements.
- (d) Establish technical and licensing approaches for the AP600 that will ultimately result in a certified design.
- (e) Assist customers in obtaining NRC approval for future plants.

Further this information has substantial commercial value as follows:

- (a) Westinghouse plans to sell the use of similar information to its customers for purposes of meeting NRC requirements for advanced plant licenses.
- (b) Westinghouse can sell support and defense of the technology to its customers in the licensing process.

Public disclosure of this proprietary information is likely to cause substantial harm to the competitive position of Westinghouse because it would enhance the ability of competitors to provide similar advanced nuclear power designs and licensing defense services for commercial power reactors without commensurate expenses. Also, public disclosure of the information would enable others to use the information to meet NRC requirements for licensing documentation without purchasing the right to use the information.

The development of the technology described in part by the information is the result of applying the results of many years of experience in an intensive Westinghouse effort and the expenditure of a considerable sum of money.

In order for competitors of Westinghouse to duplicate this information, similar technical programs would have to be performed and a significant manpower effort, having the requisite talent and experience, would have to be expended for developing analytical methods and receiving NRC approval for those methods.

Further the deponent sayeth not.

Enclosure 2



Question 440.280

Re: WCAP-14234 (LOFTRAN CAD)

Please furnish a nodalization diagram for the intended LOFTRAN model in WCAP-14234. This would be extremely helpful in evaluating the numerical effectiveness of the intended nodalization and examining the model plumbing. Also, please furnish a complete list of information on initial conditions, boundary conditions, and assumptions involved for the nodalization.

Response:

1.0 Introduction

A general nodalization diagram for the LOFTRAN representation of AP600 is supplied in Figure 440.280-1. The LOFTRAN nodalization is fixed in the computer coding to represent a general PWR configuration with the following regions:

- Reactor Vessel Region
- Hot Leg Region
- Pressurizer Region
- Steam Generator Primary Side Region
- Steam Generator Secondary Side Region
- Cold Leg Region
- Accumulators
- PRHR Region
- CMT Region

The models for each of these regions are hardwired in the coding and can not be changed without modifications to the coding. The number of nodes in many of the regions is flexible and is specified by input. More details on each of the regions are supplied in Section 3.0.

2.0 Plant Initial Conditions

LOFTRAN performs initialization calculations using input values for the parameters of Table 440.280-1 prior to performing transient calculations. Detailed distributions of initial conditions throughout the RCS and the steam generator secondary are calculated using the parameters in Table 440.280-1 and the model's constitutive thermal hydraulic equations to obtain mathematically consistent steady state conditions. For example given values for the average vessel temperature, flow rate, power and pressure, LOFTRAN will calculate the vessel temperature distribution from the inlet to the outlet. Following these calculations the initial conditions around the RCS loop are calculated. Given the steam generator primary side tube conditions, flow rates, power and the feed water temperature, then the steam generator secondary side initial conditions (steam flow, pressure, etc.) can be found.

The initial condition values used for the parameters in Table 440.280-1 are dependent upon the event being analyzed. Table 440.280-1 summarizes nominal full power plant parameters used as a basis for initial conditions. Uncertainties on these nominal parameters are factored into the initial conditions. Transients which are DNB limited use the Revised Thermal Design Procedure (RTDP) as described in Reference 1. When RTDP is used, the initial condition



uncertainties are statistically included in the DNBR safety analysis limit values and the nominal values from Table 440.280-1 are used directly.

For accidents which are not DNB limited or for which RTDP is not used, the plant initial conditions are obtained by adding the following steady state uncertainty allowances to the nominal values of Table 440.280-1:

| | |
|----------------------------------------|---------------------------------------------------------------------------------------|
| Power | ± 2 percent allowance for calorimetric uncertainty |
| Average RCS coolant system temperature | $+6.5$ °F or -7.0 °F allowance for controller dead band and uncertainty measurement |
| Pressurizer pressure | ± 50 psi for steady state fluctuations and measurement uncertainty |

At hot zero power (HZIP), the programmed average RCS temperature is 545 °F. The programmed average temperature at part power conditions varies linearly between 545 °F and the full power value given in Table 440.280-1. Nominal RCS pressure is 2250 psia at all power levels between HZIP and full power.

PRHR, CMT and other initial conditions which are input are discussed in Section 3 with the plant nodalization discussion.

3.0 Plant Nodalization

Reactor Vessel

Figure 440.280-2 shows a detailed nodalization diagram for the reactor vessel. The reactor vessel is divided into the following subregions:

- Vessel Inlet Region - The inlet region node represents the downcomer, the lower vessel head and the lower inactive (unheated) fuel region. []^{abc} nodes are used, one associated with each reactor coolant loop.
- Heated Fuel Region - The fuel is represented by two closed channel with several axial nodes in each channel. The number of axial nodes is event specific. Table 440.280-2 summarizes the number of axial nodes used for each event.
- Upper Unheated Fuel Region - This region represents the upper inactive fuel. []^{abc} nodes are used, one corresponding to each core channel.
- Outlet Plenum Region - The outlet plenum is divided into []^{abc}.





Upper Head Region - []^{abc} used in the upper head.

Under nominal conditions, cooling flow enters the upper head from the vessel downcomer and exits to the outlet plenum. At nominal conditions with full forced flow, this flow will be 1.0 % of the total vessel flow. The analyses performed with LOFTRAN are initialized assuming an initial upper head flow of 1.0 %.

At nominal full power conditions, a conservative estimate of the upper head temperature is ~571.5 °F. At hot zero power conditions, the upper head will be at the no-load temperature of 545 °F. In the analyses performed with LOFTRAN, a conservative upper or lower bound upper head temperature is used.

As an upper bound, the upper head temperature is assumed to vary linearly between 545 °F at HZP and 571.5 °F at HFP. Another 6.5 °F of uncertainty is then added. As a lower bound temperature, the vessel inlet temperature is used.

Hot Leg Region

Two hot leg regions, one for each reactor coolant loop are used. The hot leg region in each reactor coolant loop can be divided into several nodes. The number of nodes used in the hot leg is event specific and is given in Table 440.280-2.

Pressurizer Region

The pressurizer region represents the pressurizer and the surge line. []^{abc}.

The upper steam portion of the node is initialized with saturated steam, the lower portion of the node is initialized with saturated water. The initial water and steam volume assumed is dependent on the event being analyzed. Depending upon the conservative direction, an upper bound or lower bound pressurizer initial water volume is used. Figure 440.280-5 shows the minimum and maximum pressurizer water volumes used in analyses performed with LOFTRAN.

As discussed in Section 2.0, the initial pressurizer pressure is taken as 2250 psia. An uncertainty of ± 50 psi may be added depending upon the event being analyzed.

Steam Generator Primary Side Region

Independent steam generators are used for each reactor coolant loop. The primary side of each steam generator is divided into the following subregions.

- Inlet Plenum Region - The inlet plenum region represents the steam generator inlet nozzle and inlet channel head. []^{abc} used for this region.
- Tube Region - Multiple nodes are used. The number of nodes used is transient dependent and is specified in Table 440.280-2.





Outlet Plenum Region The outlet plenum region represents the outlet nozzle and outlet channel head. []^{a,b,c} used for this region.

Steam Generator Secondary Side Region

Each steam generator secondary side is modeled separately. A single node is used for the secondary side of each steam generator.

The nominal programmed steam generator water level is 525 inches above the tube sheet. Events sensitive to the initial steam generator water level use an upper or lower bound initial water level of 549 inches or 501 inches above the tube sheet. This corresponds to the programmed level $\pm 10\%$ of the instrumentation span.

The initial feedwater temperature is a function of the plant power level. The nominal feedwater temperature at hot full power is 435 °F. In the analyses performed with LOFTRAN, a ± 5 °F uncertainty is included in the initial feedwater temperature. Figure 440.280-6 shows the upper and lower bound feedwater temperature used in analyses.

Cold Leg Region

The cold leg region represents the cold leg piping and the reactor coolant pumps. A separate cold region is used for each reactor coolant loop. However, the two cold legs per RCS loop are lumped together in the LOFTRAN model. Each cold leg region in the model is broken into the number of nodes shown in Table 440.280-2.

Accumulators

The two accumulators are modeled separately. []^{a,b,c} used for each accumulator.

Of the analyses performed with LOFTRAN, the accumulators are actuated only in large steam line break transients. During steam line break transients, the accumulators inject borated fluid which mitigates the reactivity transient.

Initial accumulator conditions are used which minimize the boration ability of the accumulators. Following is a summary of the accumulator initial conditions used as compared to the nominal values.

| | <u>Value Used</u> | <u>Nominal Value</u> |
|----------------------------------------|-------------------|----------------------|
| Initial gas pressure, psia | 651.7 | 714.7 |
| Initial gas volume, ft ³ | 268 | 300 |
| Initial liquid volume, ft ³ | 1732 | 1700 |
| Initial boron concentration, ppm | 2600 | 2700 |
| Initial temperature, °F | 120 | 85 |

PRHR Region

Figure 440.280-3 shows a detailed nodalization diagram for the PRHR. The PRHR loop uses a total of []^{a,b,c} nodes. []^{a,b,c} nodes are used for the PRHR inlet piping and the inlet channel head. []^{a,b,c} nodes are





used for the heat exchanger tubes. The heat exchanger tubes are broken into 3 segments which are an upper horizontal segment ([]^{abc} nodes), a vertical segment ([]^{abc} nodes) and a lower horizontal segment ([]^{abc} nodes). The outlet channel head and piping are simulated using []^{abc} nodes.

The PRHR heat exchanger is immersed in the IRWST. []^{abc} is used to simulate the IRWST.

The IRWST is assumed to be at atmospheric pressure at the initiation of the event. Depending upon the event being analyzed, two sets of initial PRHR temperatures are used to conservatively either minimize or maximize PRHR performance.

| | Minimum PRHR <u>Performance</u> | Maximum PRHR <u>Performance</u> |
|--------------------------------------------------------------------------------|---------------------------------------|---------------------------------------|
| Initial IRWST temperature, °F | 120 | 50 |
| Initial PRHR inlet piping temperature, °F [(Nodes 1 - 3)] ^{abc} | 400 | 600 |
| Initial PRHR heat exchanger temperature, °F [(Nodes 4 - 25)] ^{abc} | 120 | 50 |
| PRHR outlet piping, °F [(Nodes 26 - 28)] ^{abc} | 120 | 50 |

CMT Region

Figure 440.280-4 shows the nodalization used for the core makeup tank loop. The CMT loop is divided into the following three subregions:

- Balance Line - This is the inlet line of the CMT. It is connected between the cold leg and the top of the CMT. []^{abc} nodes are used.
- Tank - The tank region is broken into []^{abc} fluid nodes. Associated with each fluid node is a metal node representing a section of the tank wall.
- Injection Line - The injection line is connected between the bottom of the CMT and the cold leg. []^{abc} fluid nodes are used.





Note, in the actual AP600 the injection line is connected to the direct vessel injection nozzle in the vessel downcomer. In calculating CMT flow, LOFTRAN uses the vessel downcomer pressure for the exit of the injection line, but flow is injected into the cold leg.

Depending upon the event being analyzed, two sets of initial CMT temperatures are used to conservatively either minimize or maximize CMT performance.

| | | <u>Minimum CMT Performance</u> | | <u>Maximum CMT Performance</u> | |
|-----------------------|----------------------------|--------------------------------|----------------------------------|--------------------------------|----------------------------------|
| | | Initial temperature, °F | Initial Boron Concentration, ppm | Initial temperature, °F | Initial Boron Concentration, ppm |
| Pressure Balance Line | Node [] ^{a,b,c} | 400 | RCS boron concentration | cold leg temperature | RCS boron concentration |
| | Node [] ^{a,b,c} | 120 | 3400 | 50 | 3600 |
| Tank | | 120 | 3400 | 50 | 3600 |
| Injection Line | Node [] ^{a,b,c} | 120 | 3400 | 50 | 3600 |
| | Nodes [] ^{a,b,c} | cold leg temp. | RCS boron concentration | 50 | 3600 |

References:

- 1) Friedland, A. J. and Ray, S., "Revised Thermal Design Procedure," WCAP-11397-P-A (Proprietary) and WCAP-11398-A (Nonproprietary), April 1989

SSAR Revision: NONE



| Table 440.280-1 Nominal Plant Parameters Used as a Basis for Initial Conditions in Analyses Performed With LOFTRAN | | | |
|--------------------------------------------------------------------------------------------------------------------|---------------------------------------------|---------------------------------------|----------------------------------------|
| | RTDP With 10% Steam Generator Tube Plugging | Without RTDP | |
| | | Without Steam Generator Tube Plugging | With 10% Steam Generator Tube Plugging |
| Plant Thermal Output (Mwt) | 1940 | 1940 | 1940 |
| Vessel Average Temperature (°F) | 567.6 | 565.9 | 567.6 |
| Pressurizer Pressure (psia) | 2250 | 2250 | 2250 |
| Reactor Coolant Loop Flow (GPM) | 96600 | 97100 | 94800 |
| Feedwater Temperature (°F) | 435 | 435 | 435 |





NRC REQUEST FOR ADDITIONAL INFORMATION

a, b, c



a,b,c

Figure 440.280-1 LOFTRAN Nodalization





a,b,c

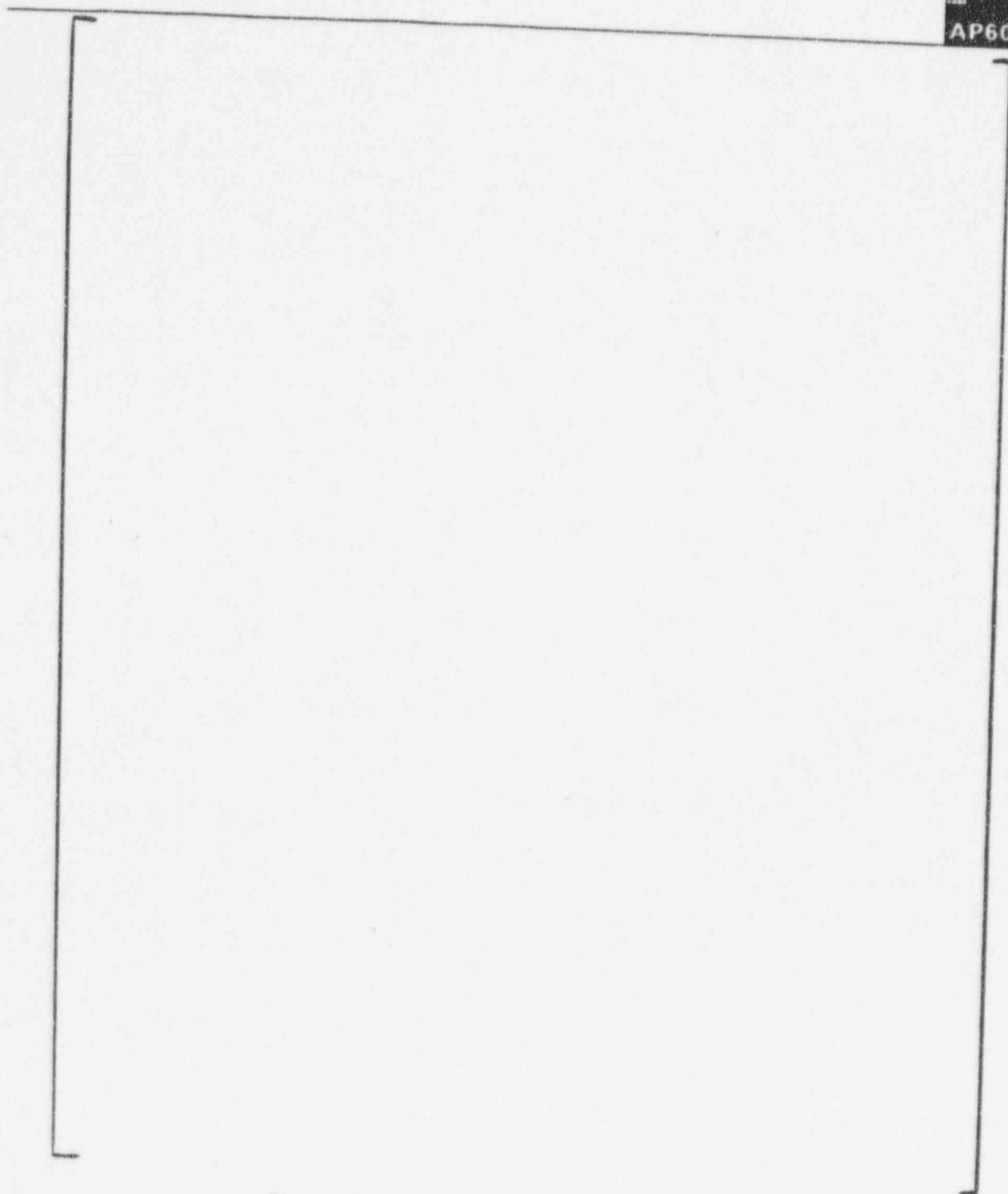


Figure 440.280-2 LOFTRAN Vessel Nodalization





a,b,c

Figure 440.280-3 LOFTRAN PRHR Nodalization



a,b,c

Figure 440.280-4 LOFTRAN CMT Nodalization



Westinghouse

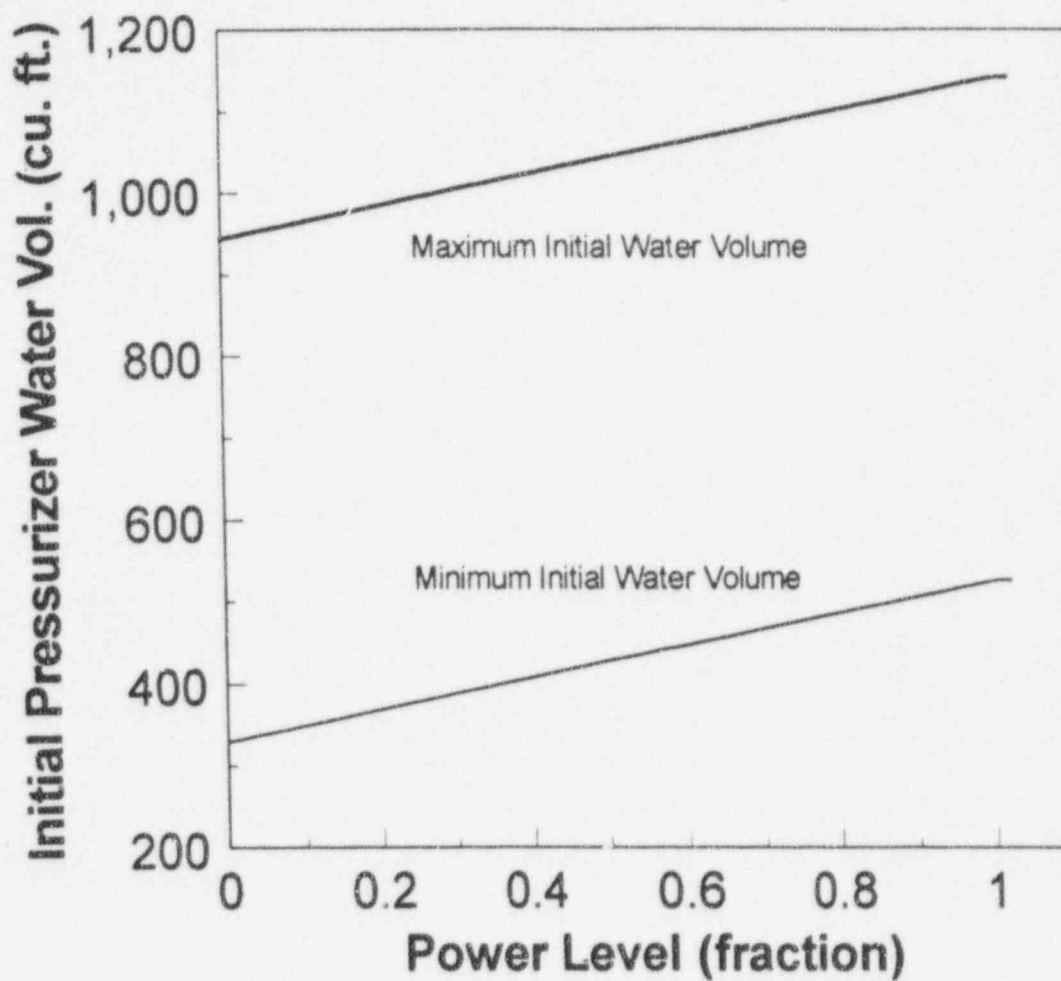


Figure 440.280-5 Initial Pressurizer Water Volume

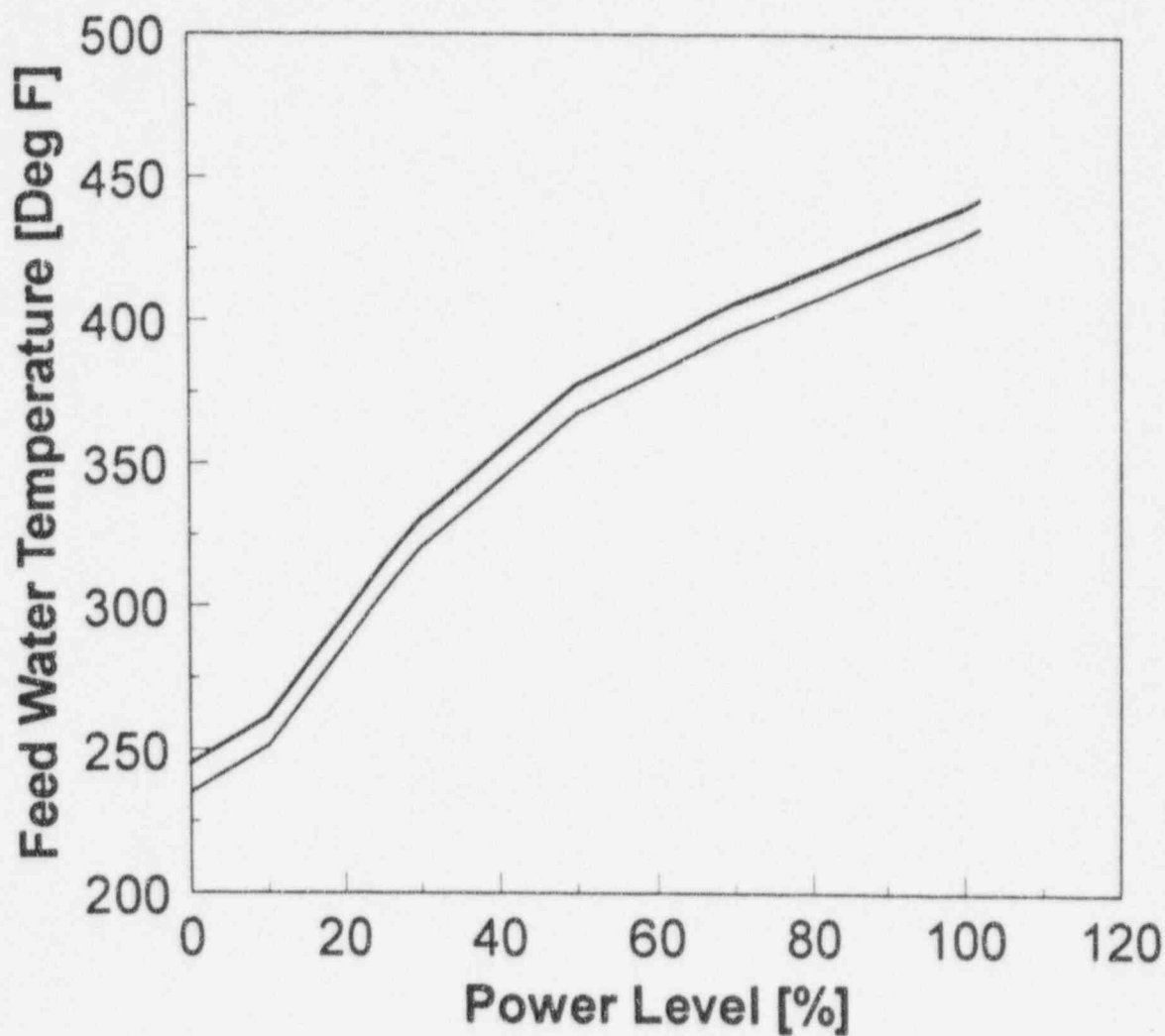


Figure 440.280-6 Initial Feedwater Temperature



Question 440.285

Re: WCAP-14234 (LOFTRAN CAD)

Section 3.1, page 3-1. Please provide a technical description of the equations, the nodalization, and numerical modelling of the CMT. Please explain whether local or global pressure is used in the CMT model and how donoring energy from the nodes to the links is performed. Also, please explain how thermal stratification (and its effect on condensation) is modelled in the CMT?

Response:

Thermal stratification and condensation concerns are already addressed in response to Question 440.320. A technical description of the equations, the nodalization, and the numerical modelling is provided hereafter.

1. Principles

The core makeup tank (CMT) model is a multi-node model that simulates the tank, the balance line connecting the reactor coolant system (RCS) cold leg with the top of the CMT, and the injection line connecting the bottom of the CMT with the reactor vessel. The thermal-hydraulics model simulates the flow in the CMT lines and tracks mass, energy, and boron concentration in the CMT. The CMT model calculations are performed explicitly from the RCS thermal-hydraulic calculations. A single CMT is simulated; to simulate the two CMTs of the AP600, flow rates out of the RCS and out of the CMT model are doubled.

Boron concentration is tracked on a node basis in the cold leg balance line and the injection line. In the CMT, boron is tracked on a tank average basis, which effectively assumes perfect mixing of the boron within the tank with fluid entering from the cold leg balance line. This assumption conservatively under predicts the boron concentration of CMT injection.

2. Nodalization

Figure 440.285-1 shows the noding used for the LOFTRAN CMT model in Chapter 15 SSAR analyses. Fluid noding in the CMT model is as follows:

- []^{abc} nodes in the CMT tank
- []^{abc} nodes in the injection line
- []^{abc} nodes in the balance line between the cold leg and the CMT

Heat transfer from the tank fluid through the walls of the tank is simulated and []^{abc} metal nodes ([]^{abc} for each fluid node) are used.





3. Description of the equations

3.1 Flow Calculations

Flow calculations in the CMT injection line and the cold leg connection are made explicitly from the main RCS calculations done in LOFTRAN. As boundary conditions to the CMT model, the following pressures from the main RCS loop are used to calculate the CMT line flow rates:

| | | |
|--------------|---|-------------------------------------------------------------|
| P_{VESSEL} | = | pressure at CMT injection point in reactor vessel downcomer |
| P_{CL} | = | pressure in cold leg where the balance line connects |

In calculating the flow rates in the injection line and the cold leg balance line, the following general momentum equation is used:

$$\frac{dw}{dt} = g_c \frac{\left(\Delta P_{Driving} - K \frac{w^2}{\rho} \right)}{L/A} \quad 440.285-1$$

where:

| | | |
|----------------------|---|------------------------------------------------------------------------------------------------------------|
| dw/dt | = | rate of change in mass flow rate, lbm/sec ² |
| $\Delta P_{Driving}$ | = | driving pressure, lbf/ft. ² |
| g_c | = | gravity acceleration, lbm-ft./lbf-sec ² |
| L/A | = | inertial length (length/area derived from user input volumes and flow areas), 1/ft. |
| K | = | pressure loss coefficient (user input values), (lbf/ft. ²)/((lbm/sec) (ft. ³ /sec)) |
| w | = | mass flow rate, lbm/sec |
| ρ | = | fluid density, lbm/ft. ³ |

Driving pressure ($\Delta P_{Driving}$) is calculated using:

$$\Delta P_{Driving} = P_{CL} - BH_{BL} + BH_{TANK} + BH_{IL} - P_{VESSEL}$$

In calculating the CMT line flow rates, the driving pressure (buoyancy head) in several regions (injection line, cold leg balance line, and the CMT) is used. As discussed previously, each of these regions is divided into several nodes. The buoyancy head in each region is calculated as:





$$BH_{\text{region}} = \sum_{i=1}^n \rho_i h_i$$

440.285-2

where:

| | | |
|----------------------|---|----------------------------------------------------|
| BH_{region} | = | Buoyancy (elevation) head difference in the region |
| region | = | BL - balance line between cold leg and CMT |
| | | TANK - CMT |
| | | IL - injection line between CMT and vessel |
| ρ_i | = | fluid density in node i |
| h_i | = | height of node i |
| n | = | number of nodes in the region |

For the purpose of calculating fluid thermal hydraulic properties, a global pressure is used for the CMT model. The global pressure used corresponds to the top of the CMT. The global pressure is calculated from the pressure in the cold leg where the balance line connects using:

$$P_{\text{CMT}} = P_{\text{CL}} - BH_{\text{BL}} - K_{\text{BL}} \frac{w^2}{\rho}$$

440.285-3

where:

| | | |
|------------------|---|----------------------------------------------------------------------------------|
| P_{CMT} | = | Pressure at the top of the CMT used as global CMT pressure for fluid properties. |
| K_{BL} | = | pressure loss coefficient for the balance line between the cold leg and the CMT. |

During non-LOCA transients, the CMT will operate in water recirculation mode. The draindown injection mode of operation does not occur during non-LOCA events. However, after long-term operation of the CMT, the CMT temperature will be elevated. If the RCS is depressurized to the saturation temperature of fluid in the CMT, then flashing may occur in the CMT line. The CMT model uses homogeneous nodes and stratification of the steam in the upper region of the cold leg line will not be simulated. The effect of any potential stratification is accounted for by applying a penalty to the buoyancy head of the cold leg balance line.

Boiling is detected if the water subcooling in the balance line or CMT is smaller than a prescribed user input value. Flashing is assumed to occur if the following is true:

$$T_{\text{sat}} - T_{\text{node } i} < D_{\text{CMT sat}}$$

where:

| | |
|--------------------|--------------------------------------------------|
| T_{sat} : | water saturation temperature at the CMT pressure |
|--------------------|--------------------------------------------------|





$T_{node\ i}$: water temperature in the node i
 $D_{cmt\ sat}$: subcooling limit (input parameter)

If boiling is detected or if the subcooling limit is exceeded, the potential steam accumulation at the CMT pipe top is taken into account by a penalty on the cold leg to CMT balance line buoyancy (BH_{BL}) calculation. Assuming that there is only steam in the vertical pipe portion at the CMT top, the buoyancy is increased by the following quantity:

$$\text{Penalty} = H_{bub} (\rho_{bal} - \rho_{steam}) / 144$$

where:

H_{bub} : Equivalent height of the stratified zone. Value is set as input.
 A realistic calculation may be done with the descending length of the inlet CMT pipe.
 A very conservative calculation may be done with a larger value that which stops the natural circulation as soon as boiling is detected.

ρ_{bal} : mixture density in the cold leg to CMT line top node.
 ρ_{steam} : saturation steam density at the CMT pressure.

The penalty model was developed to prevent using LOFTRAN in an area where it's physical modelling is not appropriate. The penalty term was introduced to offer the possibility to perform conservative calculations if boiling is detected. A high penalty term stops CMT natural circulation as soon as boiling is detected.

3.2 Convective Heat and Mass Transfer Calculations

Mass and energy transfer to and from a node is computed assuming a single phase fluid with a uniform velocity profile which moves as a slug. A generalized modular routine is used for this "slug flow" model throughout the LOFTRAN hydraulic model. Given initial node fluid conditions and average input to a node (flow, enthalpy) over some time of interval, the "slug flow" routine computes final fluid conditions based on single phase fluid with a uniform velocity profile which moves as a slug. Detailed equations and the numerical modelling of the "slug flow" routine are provided in section 4.2 of the answer to this question.

The LOFTRAN model of the CMT loop consists of the balance line, the CMT and the injection line. As identified in Section 2, the CMT loop is divided into numerous nodes. The "slug flow" model is used to compute the mass and energy transfer from node to node.

Calculations are performed node by node, starting from the first node of the balance line, which is in contact with the RCS cold leg. The calculation of the first balance line node uses the CMT loop flow calculated by equation 440.285-1 and the enthalpy of the connection point in the RCS cold leg, as a boundary condition.





3.3 Boron Transport Calculations

In general, boron transport from node to node in the LOFTRAN hydraulic model is calculated using a companion routine to the "slug flow" model. Hereafter this routine will be referred to as the "boron slug flow" model.

Given initial node boron concentration and fluid conditions and the average input to a node of flow and boron over some time of interval, the "boron slug flow" routine computes final fluid conditions based on single phase fluid with a uniform velocity profile which moves as a slug. Detailed equations and the numerical modelling of the "boron slug flow" routine are provided in Section 4.3 of the answer to this question.

The boron concentration in the balance and injection line nodes is computed using the generalized LOFTRAN "boron slug flow" routine. The boron concentration at the balance line inlet (boundary condition) is equal to the RCS boron concentration of the cold leg node where the balance line is connected.

The boron concentration within the CMT is not calculated using the "boron slug flow" model. To conservatively under predict the boron concentration exiting the CMT, the CMT boron concentration is computed assuming perfect mixing of the boron in the []^{abs} nodes of the CMT. The following equations are used for the calculation of the CMT boron concentration.

$$\frac{d M_{B_{CMT}}}{dt} = -C_{B_{CMT}} \times W_{IL} + C_{B_{BL}} \times W_{BL} \quad 440.285-4$$

$$C_{B_{CMT}} = \frac{M_{B_{CMT}}}{M_{W_{CMT}}} \quad 440.285-5$$

Where :

$M_{B_{CMT}}$ = mass of boron in the CMT (lbm)

$M_{W_{CMT}}$ = mass of water in the CMT (lbm)



Westinghouse



$C_{B_{CMT}}$ = boron concentration in the CMT (lbm of boron per lbm of water)

$C_{B_{BL}}$ = boron concentration at the balance line exit (lbm of boron per lbm of water)

W_{IL} = mass flow rate at the inlet of the injection line (lbm/sec)

W_{BL} = mass flow rate at the balance line exit (lbm/sec)

3.4 Heat Transfer Between Water and CMT Wall

Heat transfer from the tank fluid to the tank metal wall and from the tank metal wall to the containment air is simulated. There are []^{abc} metal nodes used for the tank wall (one metal node for each fluid node). Axial conduction between the tank metal nodes is neglected. Heat transfer is calculated using the following equations.

$$M_{Metal_i} \times C_p \times \frac{dT_{Metal_i}}{dt} = -UA_{Inner_i} (T_{Metal_i} - T_{Water_i}) - UA_{Outer_i} (T_{Metal_i} - T_{Air}) \quad 440.285-6$$

$$M_{Water_i} \times \frac{dH_{Water_i}}{dt} = UA_{Inner_i} (T_{Metal_i} - T_{Water_i}) \quad 440.285-7$$

Where:

M_{Metal_i} = mass of metal in ith CMT metal node, lbm

C_p = heat capacity of the CMT metal, Btu/lbm/°F





- M_{Water_i} = mass of water in ith CMT fluid node, lbm
- H_{Water_i} = water enthalpy in ith CMT fluid node, Btu/lbm
- UA_{Inner_i} = heat transfer coefficient times the surface area between the ith CMT fluid node and ith metal node, Btu/sec-°F
- T_{Metal_i} = temperature of the ith CMT metal node, °F
- T_{Water_i} = temperature of the ith CMT fluid node, °F
- UA_{Outer_i} = heat transfer coefficient times the surface area between the CMT ith metal node and the containment atmosphere, Btu/sec-°F
- T_{air} = containment temperature, °F
- t = time, seconds





4. Numerical Modelling

The equations presented in section 3 are solved at each CMT internal time step as described hereafter. In the following, t is the current time (i.e. the time at the end of the time step) and Δt is the time step in seconds.

4.1 Solve Momentum equation (Equation 440.285-1)

CMT flow is calculated using the momentum equation and the "slug flow" model. Flow from the RCS into the CMT balance line is calculated using the momentum equation (Equation 440.285-1). The momentum equation is numerically solved using the following:

$$w^t = w^{t-\Delta t} + \Delta t g_c \frac{\Delta P_{Driving}^{t-\Delta t} - K \frac{(w^{t-\Delta t})^2}{\rho}}{L/A}$$

Once the flow (w) into the first CMT balance line node is calculated, the "slug flow" model is used to calculate the flow from node to node throughout the CMT loop. Calculations with the "slug flow" model are performed node by node starting with the first balance line node. The numerics of the "slug flow" model are shown in the following section.

4.2 Convective Mass and Heat Transfer Using the "Slug Flow Model"

In the "slug flow model", mass and energy transfer to and from a node is based on a single phase fluid with a uniform velocity profile which moves as a slug. Referring to Figure 440.285-2, given the node initial conditions and the average input to the node over the time step, the node fluid conditions at the end of the time step and the fluid exiting the node are calculated using the following equations:

- For an unheated node ($Q = 0.0$) and $V_{in} \geq V_j$

$$h_j(t) = h_{in}$$

$$m_j(t) = V_j \rho$$

where:

ρ is the fluid density evaluated at the current pressure $P(t)$ and an enthalpy of h_0 . The enthalpy of the fluid in the node, h_0 is evaluated as:





$$h_0 = h(t - \Delta t) + \frac{V_j [P(t) - P(t - \Delta t)] \frac{1 \text{ ft}^2}{144 \text{ in}}}{m_j(t - \Delta t) \frac{777.98 \text{ ft lbf/BTU}}{m_j(t - \Delta t)}}$$

- For an unheated node ($Q = 0.0$) and $V_{in} < V_j$

$$h(t) = \frac{M_{in} h_{in} + M_0 h_0}{M_{in} + M_0}$$

where

$$M_0 = (V_j - V_{in}) \rho$$

ρ is the fluid density evaluated at the current pressure $P(t)$ and an enthalpy of h_0 .

- For a heated node ($Q \neq 0.0$) and $V_{in} \geq V_j$

$$h_j(t) = h_{in} + \frac{Q}{2 M_{in}}$$

$$m_j(t) = V_j \rho$$

where ρ is the fluid density at the final pressure $P(t)$ and an enthalpy of $h_j(t)$

- For a heated node ($Q \neq 0.0$) and $V_{in} < V_j$





$$h(t) = (h(t - \Delta t) + \Delta h) \left(1 - \frac{V_{in}}{V_j} \right) + \frac{V_{in}}{V_j} h'$$

where

$$\Delta h = \frac{\frac{Q}{2} - M_{in} (h_j(t - \Delta t) - h_{in})}{M_o}$$

$$h' = h_{in} + \frac{Q}{2 M_{in}}$$

Final mass in the node is computed from the equation of state:

$$m_j(t) = V_j \rho(h(t), P(t))$$

Exit mass flow is computed by conservation of mass and exit enthalpy is computed by conservation of energy.

The slug model assumes uniform enthalpy throughout the node. For this reason, the model yields a true delay only for exact volume replacement for each time interval. For inlet flows less than replacement, the final enthalpy is computed as a volume-density weighted average of the inlet enthalpy and the initial fluid enthalpy. Effectively, this produces mixing within the section. For high flow, (node fluid more than replaced) the final enthalpy is dependent only upon the flow into the node. However, mixing occurs since only the average exit enthalpy over a time step is computed. No attempt is made to calculate slip.





4.3 Boron Transport Using the "Boron Slug Flow Model"

Referring to Figure 440.285-2, the boron slug flow model calculates the boron concentration in a node given the average input of flow and boron concentration over some time interval, based on slug flow as discussed in Section 4.2. The following equations are used:

- For $M_{in} \geq m_j(t)$

$$Cb_j(t) = Cb_{in}$$

- For $M_{in} < m_j(t)$

$$Cb_j(t) = \frac{M_{in} Cb_{in} + (m_j(t) - M_{in}) Cb_j(t - \Delta t)}{m_j(t)}$$

Boron concentration of the flow out of the node is computed to conserve boron using:

$$M_{out} Cb_{out} = m_j(t - \Delta t) Cb_j(t - \Delta t) - m_j(t) Cb_j(t) + M_{in} Cb_{in}$$

or

$$Cb_{out} = \frac{m_j(t - \Delta t) Cb_j(t - \Delta t) - m_j(t) Cb_j(t) + M_{in} Cb_{in}}{M_{out}}$$





4.4 Heat Transfer Between Water and CMT Wall Numerical Modeling

Equations 440.285-6 and 440.285-7 are solved explicitly. The heat transfer over a time step from the fluid CMT node to the CMT metal node is calculated using:

$$Q_{Inner_i} = UA_{Inner_i} (T_{Metal_i}^{(t-dt)} - T_{Water_i}^{(t-dt)}) dt$$

The heat transfer between the CMT metal node and the containment atmosphere is similarly calculated using:

$$Q_{Outer_i} = UA_{Outer_i} (T_{Metal_i}^{(t-dt)} - T_{air}^{(t-dt)}) dt$$

The metal node temperature and the water enthalpy are updated using:

$$T_{Metal_i}^{(t)} = T_{Metal_i}^{(t-dt)} - \frac{(Q_{Inner_i} + Q_{Outer_i})}{MCp_i}$$

$$H_{Water_i}^{(t)} = H_{Water_i}^{(t-dt)} + \frac{Q_{Inner_i}}{M_{Water_i}}$$

where :

$T_{Metal_i}^{(t)}$ = metal node temperature at time equal to t, °F

$T_{Metal_i}^{(t-dt)}$ = metal node temperature from the previous time step at time equal to t - dt, °F

$H_{Water_i}^{(t)}$ = fluid node enthalpy at time equal to t, °F





$H_{Water_i}^{(t-dt)}$ = fluid node enthalpy from the previous time step at time equal to $t - dt$, °F

MCp_i = metal node heat capacity, Btu/°F

The metal node inside and outside heat transfer coefficient time surface areas and metal node heat capacity are code input parameters. Values may be entered for each of the []^{abc} metal nodes. The containment atmosphere temperature is also a code input parameter.

References

- 440.285-1 LOFTRAN-AP and LOFTTR2-AP Final Verification and Validation Report. WCAP-14308, June 95
- 440.285-2 LOFTRAN & LOFTTR2 AP600 Code Applicability Document. WCAP-14234, November 1994

SSAR Revision: NONE



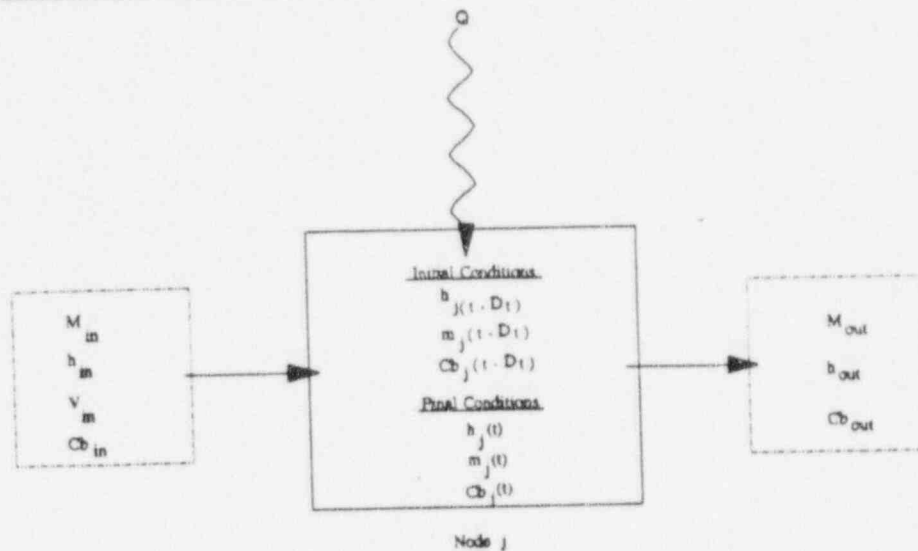


a,b,c

Figure 440.285-1 CMT Nodalization



Westinghouse



| | | |
|---------------------|---|-----------------------------------------------------------------------------|
| t | = | time at the end of the time step, seconds |
| Δt | = | time step size, seconds |
| $t-\Delta t$ | = | time at the beginning of the time step, seconds |
| $P(t)$ | = | pressure at the end of the time step, psia |
| $P(t-\Delta t)$ | = | pressure at the beginning of the time step, psia |
| $h_j(t)$ | = | enthalpy of fluid in node j at the end of the time step, BTU/lbm |
| $h_j(t - \Delta t)$ | = | enthalpy of fluid in the node at the beginning of the time step, BTU/lbm |
| h_{in} | = | enthalpy of fluid being added to the node, BTU/lbm |
| h_{out} | = | enthalpy of fluid exiting the node, BTU/lbm |
| $m_j(t)$ | = | mass of fluid in node j at the end of the time step, lbm |
| $m_j(t - \Delta t)$ | = | mass of fluid in the node j at the beginning of the time step, lbm |
| M_{in} | = | mass being added to the node over the time step, lbm |
| M_{out} | = | mass of fluid exiting the node, lbm |
| $Cb_j(t)$ | = | boron concentration in node j at the end of the time step, ppm |
| $Cb_j(t-\Delta t)$ | = | boron concentration in node j at the beginning of the time step, ppm |
| Cb_{in} | = | boron concentration of fluid being added to the node, ppm |
| Cb_{out} | = | boron concentration of fluid exiting the node, ppm |
| V_j | = | volume of node j, ft ³ |
| V_{in} | = | volume of fluid being added to the node over the time step, ft ³ |
| Q | = | heat addition to the node over the time step, BTU |

Figure 440.285-2 Slug Flow Model

NRC REQUEST FOR ADDITIONAL INFORMATION



Question 440.290

Re: WCAP-14234 (LOFTRAN CAD)

Please explain how time step control is accomplished between the CMT and the RCS. Do the results remain stable for continually decreasing the time step? Please provide substantiation.

Response:

The methodology used to control the time step between the RCS and the CMT module is explained in the response to RAI 440.291.

As mentioned in the response to RAI 440.286, the time step influence on the CMT model response was analyzed in Reference 440.290-1. The CMT Test C064506 (Matrix Test 506) was selected and the conclusion was that the response is independent of the CMT time step for time steps in the range of 2.5 seconds or less.

References:

440.290-1 WCAP-14307, "AP600 LOFTRAN-AP and LOFTTR2-AP Final Verification and Validation Report," June 1995

SSAR Revision: None



Westinghouse

440.290-1

NRC REQUEST FOR ADDITIONAL INFORMATION



Question 440.302

Re: WCAP-14234 (LOFTRAN CAD)

Section 3.1. Please show how the metal heat transfer is incorporated into the numerical solution of the energy equation of the CMT.

Response:

A detailed description of the equations, the nodalization, and the numerical modeling used for the CMT heat and mass transfer calculations, including the heat transfer between the water and the CMT wall, is provided in the response to RAI 440.285.

SSAR Revision: None



Westinghouse

440.302-1



Question 440.314

Re: LOFTRAN Code Applicability Document (CAD)

Section 3.1. How was the noding for the CMT arrived at? Were any noding sensitivity studies performed? Please explain.

Response:

The CMT model was developed with a relatively large number of nodes (15 nodes) to allow for detailed modelling of condensation at the top of the CMT that would result if a steam space formed. The CMTs remain water solid during the SSAR non-LOCA and SGTR transients so this detail is not required. This physical behavior is confirmed by the SPES-2 results and well predicted by the LOFTRAN code (Reference 440.314-1). Noding sensitivities were performed on CMT Matrix Test 506 and presented in Reference 440.314-1, which concluded that the sensitivity to the CMT noding is relatively small and that a model with nodes of equal size provides a good prediction of the CMT water temperature profile evolution.

References

440.314-1 WCAP-14307, LOFTRAN-AP and LOFTTR2-AP Final Verification and Validation Report, June 1995

SSAR Revision: NONE



Question 440.460

Re: AP600 LOFTRAN-AP and LOFTTR2-AP Final Verification and Validation Report

(a) CMT Flow, page 5-29: States "There were no significant differences in the flow rates in the CMTs." Examination of Figure 5.5.2-12 shows very small flow rates, around 0.1 lbm/sec for the CMT's. There is a difference in the flow rates out about 3000 seconds into the transient. How does this difference scale to the AP600? The difference is about 0.015 lbm/sec for the average, or about 12-13%. Please show that the difference will not increase for the AP600 to justify modeling the two CMTs as one.

(b) Page 5-180: CMT Flow: It is stated that the CMT flow is shown in Figure 5.5.4-50. Please provide this figure.

(c) There is CMT flow shown in Figure 5.5.4-42. Asymmetric behavior is shown for Test 11, Run 2. Please explain this apparent contradiction to the argument that two CMTs can be modeled as one. Also, please provide larger scale plots of the comparisons to the experimental data.

Response:

Response to (a):

See response to RAI 440.283 which discusses the justification for employing the LOFTRAN model with one CMT to analyze the two CMTs in the AP600. There are no design basis events analyzed with LOFTRAN which use the CMT for mitigation where asymmetric conditions occur in the cold legs affecting CMT performance. In the response to that RAI, it is acknowledged that the CMT injection flow rates may differ due to differences in piping layouts, initial condition variations, and hardware uncertainties. In order to perform conservative, bounding analyses, limiting characteristics are selected on an event by event basis. In the AP600, the CMT discharge lines contain orifices which are used to equalize the overall line resistances of both CMTs such that they both are within a design tolerance. Included in the ITAACs are CMT tests to demonstrate that the line resistances are within a certain tolerance of each other. In the SPES-2 test facility the resistance of the injection line of the two CMTs differs by []^{abc} percent (Reference 440.460-1). It is therefore expected that the two CMTs in the SPES-2 facility will produce different injection flow rates, and that the LOFTRAN model, using maximum line resistances for all calculations (except for Run 4 of Test 10) would not exactly match the test results. In the test both CMTs behave similarly. Although the flow rates differ due to the different line resistances, the trends are consistent. This demonstrates that the RCS conditions will not result in different trends in the injection flow from the CMTs. The LOFTTR2-AP calculations of the lumped CMT compare well with the total experimental injection flow rate.

Run 4 was presented in the V & V report to show the sensitivity to the CMT line resistance. The []^{abc} percent reduction in the LOFTRAN input CMT line resistances induced an increase of flow injected by the CMTs of about []^{abc} percent. Based on this sensitivity the [20]^{abc} percent difference in the SPES-2 injection line resistances could readily account for about []^{abc} percent of the difference in injection flow rates. Figure 440.460-1 was generated using the experimental results for the two CMT injection flows (from Figure 5.5.2-12 in the V & V report) with the flow in the CMT in Loop B increased by []^{abc} percent to show how the flows would be expected to compare had the line resistances been closer. This confirms that had the line resistances been closer, as they will for the AP600,





the difference in injection flow between the two CMTs would be less than 1 percent. A difference of this magnitude is accommodated in AP600 analyses by using bounding input assumptions.

Response to (b):

The reference to Figure 5.5.4-50 (on page 5-180 of the V & V report) for the CMT flow from Test 11 Run 2 is incorrect. The data is plotted in Figure 5.5.4-42 (page 5-228 of the V & V report).

Response to (c):

Figures 440.460-2 and 440.460-3 present the CMT flow data shown in Figure 5.5.4-42 of the V & V report with the scale modified to allow for more detailed observation. Figure 440.460-2 compares the experimental results for the two CMTs. The difference in the injection flow from the two CMTs is not significant and can be attributed to the differences in the line resistances and the accuracy of the measurements. Figure 440.460-3 compares the total experimental injection flow from the CMTs to the LOFTTR2-AP calculated total injection flow.

For approximately the first 20 seconds of CMT injection, the experimental results show a significantly larger injection flow rate than is predicted by LOFTTR2-AP. This difference is caused by the model input used to simulate the contribution of the primary system flow to the total static head difference across the CMTs. During this period of time the reactor coolant pumps (RCPs) continue to provide forced primary system flow. The LOFTTRAN-AP and LOFTTR2-AP codes include terms to simulate the net pressure changes from the outlets of the RCPs to DVI nozzle locations. This allows for proper boundary conditions to be calculated for the CMT, even though the code actually models CMT injection into the cold legs. The experimental results demonstrate that in the SPES-2 test facility, forced flow conditions (in contrast to natural circulation) produce an increased pressure drop between the RCPs and the injection point, leading to the observed increase in CMT injection flow. The LOFTTR2-AP input that models this pressure drop was not tuned to match the SPES-2 downcomer configuration, since the RCPs are tripped on a CMT actuation signal (plus delay time). The brief period when CMTs are actuated and RCPs are still running is not significant to the safety analysis. The pressure differential is a function of the square of the flow, so that once the RCPs trip, the pressure drop is substantially reduced and the predicted and experimental flows converge.

References:

440.460-1 WCAP-14309, AP600 Design Certification Program SPES-2 Tests Final Data Report, March 1995.

SSAR Revision: NONE



NRC REQUEST FOR ADDITIONAL INFORMATION



Figure 440.460-1 Test S01110 - CMT Flow

— Experimental Results Loop A
----- Experimental Results Loop B Increased By 9%

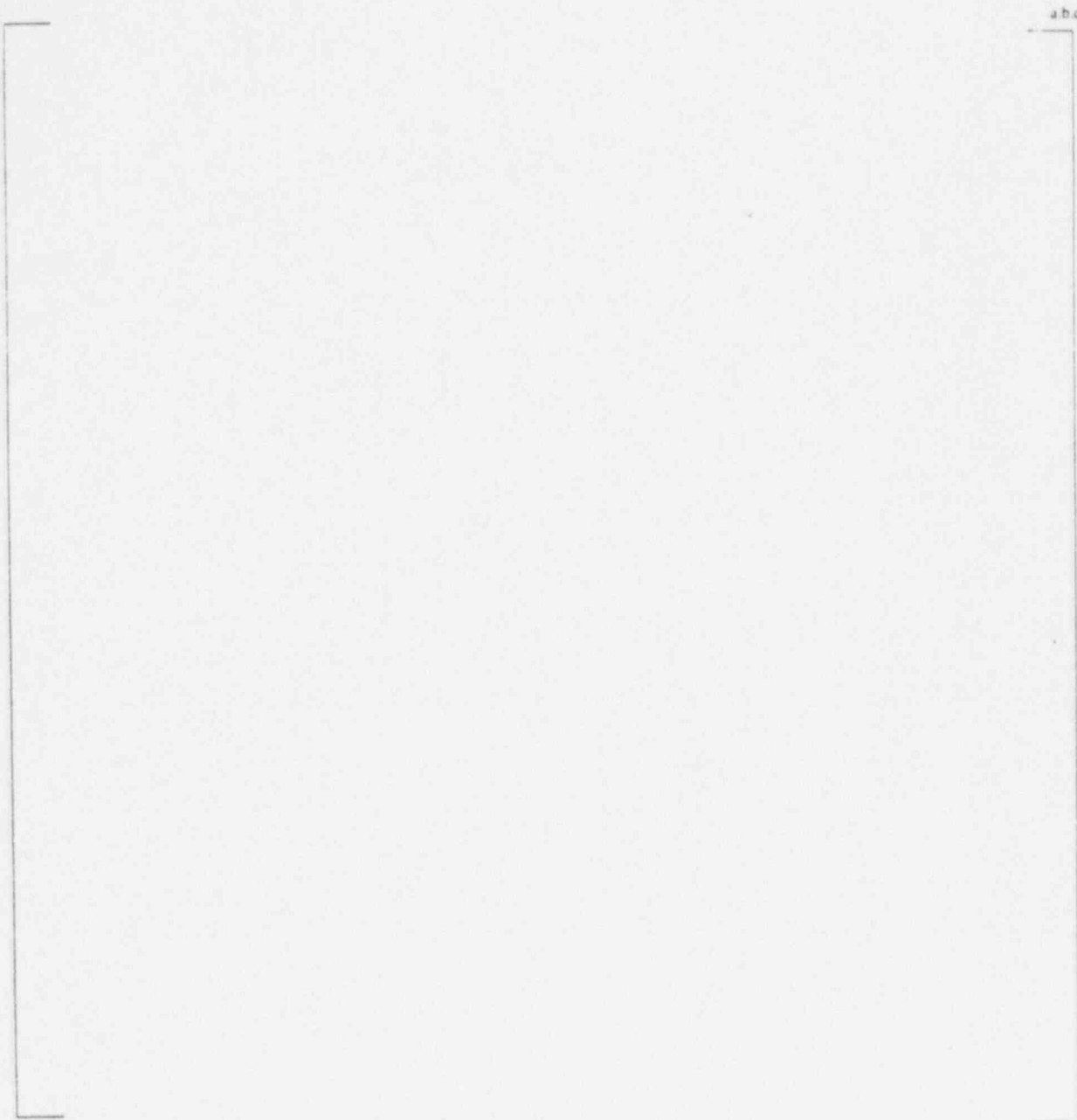


Figure 440.460-2 Test S01211 - CMT Flow

————— Experimental Results Loop A
 - - - - - Experimental Results Loop B



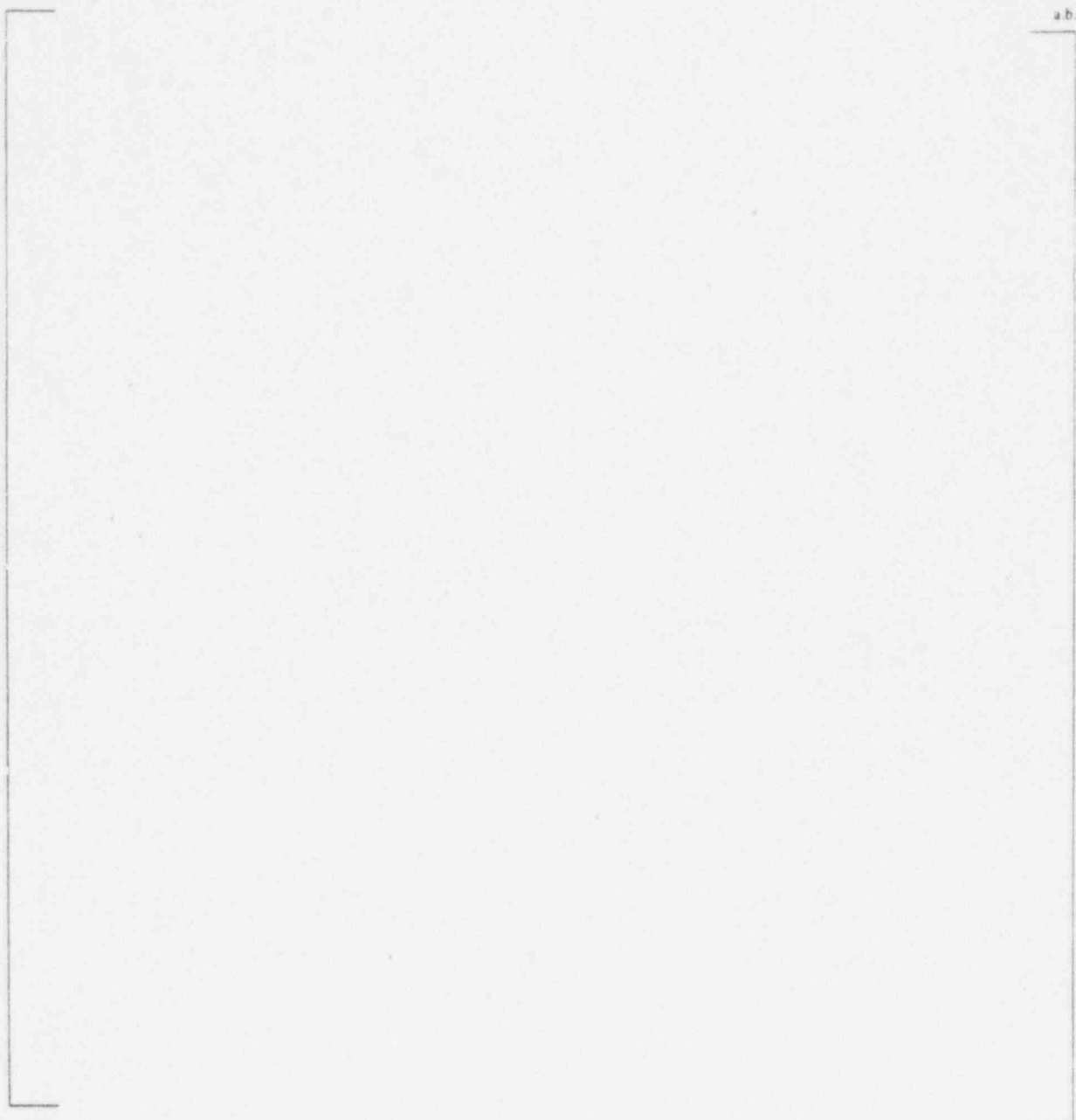


Figure 440.460-3 Test S01211 - CMT Flow

— Experimental Results Loop A + Loop B
----- LOFTTR2-AP Calculation Total



Westinghouse



Question 440.542

Re: NOTRUMP PVR FOR OSU TESTS, LTCT-GSR-004, SEPTEMBER 1995

Figure 5.2-12 displays an overprediction of the downcomer liquid level as calculated by the NOTRUMP code. Explain the reasons for this non-conservative result, since the additional downcomer inventory will also produce a higher inventory in the inner vessel containing the core and upper plenum. Also, explain the reasons for the high frequency oscillations in the downcomer level from about 1000 to 1600 seconds.

Response:

Figure 440.544-1 shows that the downcomer collapsed liquid level in the OSU test is consistently lower, by an average of 8 inches, than the NOTRUMP prediction between about 500 and 1400 seconds. The NOTRUMP simulation exhibits similar behavior to the test, albeit with a time shift arising from the plateau in primary circuit pressure (Reference, RAI 440.541). The NOTRUMP simulation predicts actuation of all ADS stages approximately 300 seconds later than the test. This results in delayed accumulator and IRWST injection. During the period of time when the primary circuit pressure is constant the boil-off rate is matched by the draining rate of CMT-2. In the absence of accumulator injection the pseudo steady state situation results in a lower primary circuit inventory for a sustained period from 500 to about 850 seconds, during which the prediction of liquid level in the downcomer is higher and the core collapsed level is lower than test data.

Therefore, the time shift in the NOTRUMP simulation leads to some conservatism in the mass inventory in the event of modest overprediction of the downcomer level. The NOTRUMP simulation of the downcomer level after the 300 second time shift, ie. from about 800 seconds compared with the test data from 500 seconds, does not produce non-conservative predictions of the core level taking account of the 300 second time shift, Figure 440.544-2 (Reference, 440.554-1).

The oscillations in downcomer level from about 1000 seconds are due to the fluctuating ADS stage 4 flow during that period. These oscillations are of the order of 1 ft in magnitude, similar magnitude oscillations are observed in the core collapsed liquid level prediction.

References

440.542-1 Response to RAI 440.547, December, 1995

SSAR Revision: NONE





Downcomer Collapsed Liquid Level

— Test Data (SB09)

— NOTRUMP Simulation

(a,b,c)

Figure 440.542-1





Core Collapsed Liquid Level

— Test Data (SB09)

— NOTRUMP Simulation

(a,b,c)

Figure 440.542-2



Westinghouse

440.542-3



Question 440.547

Re: NOTRUMP PVR FOR OSU TESTS, LTCT-GSR-004, SEPTEMBER 1995

Provide the NOTRUMP collapsed liquid level transient in the core/upper plenum for this break. Also, provide the mixture level transient in the upper plenum and core void fraction transients for the four core nodes for this event. Show the fluid level plots in the downcomer and inner vessel (lower plenum, core, upper plenum) for this event. Also, provide the steam release rate from the two-phase surface for this transient.

Response:

The requested plots for the core levels and void fractions are contained in the response to RAI 440.492.

The steam release rate from the two-phase surface from NOTRUMP is not currently available, however, the core exit mass flow rate for steam only is available and is provided in Figure 440.547-1 for comparison. The agreement is adequate if the NOTRUMP predictions from approximately 500 to 800 seconds are discounted due to the plateau in the pressurizer pressure (discussed in response to RAI 440.541) which is not a feature of the test data.

SSAR Revision: NONE



Westinghouse



Steam Flow Rate at Core Exit

— Test Data (SB09)
— NOTRUMP Simulation

(a,b,c)



Figure 440.547-1





Question 440.553

Re: NOTRUMP Preliminary Validation Report for SPES-2 Tests (PXS-GSR-002, July 1995)

Provide the ADS valve mass flow rate comparisons with the test data for the transients listed in the NOTRUMP Validation Report for the SPES-2 Tests presented in PXS-GSR-002. Provide the ADS valve mass flow rates for the DVI line breaks as the first priority, and the remaining cases as follow on.

Response:

The requested comparisons of the ADS valve mass flow rates are presented in Figures 440.553-1 to 440.553-16. Both instantaneous mass flow rates and mass flows integrated with time are presented. The NOTRUMP mass flow rates, and their integrals, represent the total liquid and vapor flow. The SPES-2 data is as presented in Reference 440.553-1. In the SPES-2 facility, the integrated mass flow was measured using catch tanks with condensers, so that the total discharge inventory is measured. Mass flow rates have been derived from the measured mass by time point to time point differentiation. To reduce the level of noise, the mass flow rates were derived from the mass data by using an average of 141 mass measurements centered on the current and previous times, in the calculation. This averaging process means the derived flows appear to start earlier, and end later (by as much as 35 seconds) than reality. The derived mass flow rates will also tend to have smeared representations of the variations, so that peak mass flow rates will be under predicted. The integrated mass data is a direct measurement and thus provides a better result for comparison with NOTRUMP.

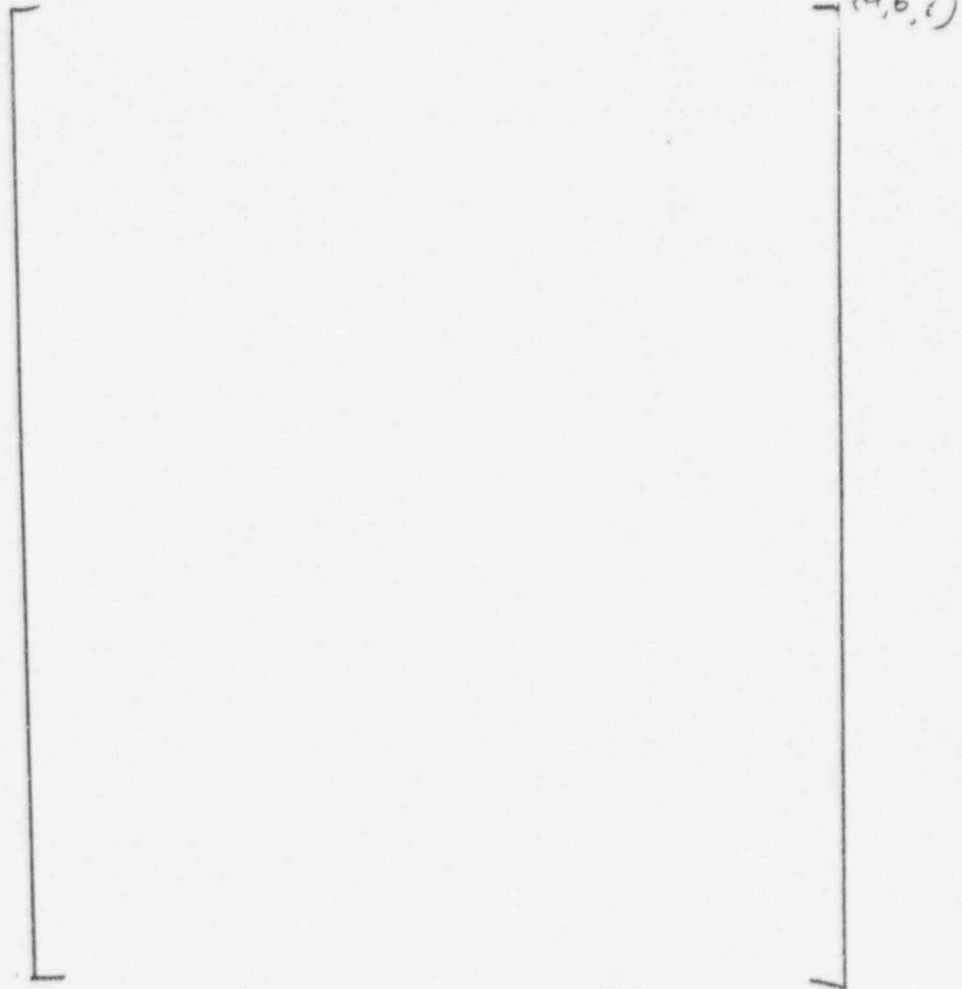
It should be noted that for test S00706, the double ended DVI line break, the ADS 4 catch tank was used to weigh inventory from the CMT side of the break, as well as the inventory discharged via the ADS 4 valves. All flow before the initiation of ADS 4 should thus be ignored in Figure 440.553-11. The integrated flow plotted in Figure 440.553-12 has been adjusted to allow for the mass of water in the catch tank at the time of ADS 4 actuation in order to allow a better comparison with the NOTRUMP results.

The code results are close to the test data for some of the cases, but higher for other cases. These differences will be investigated further prior to the NOTRUMP Final V&V Report.

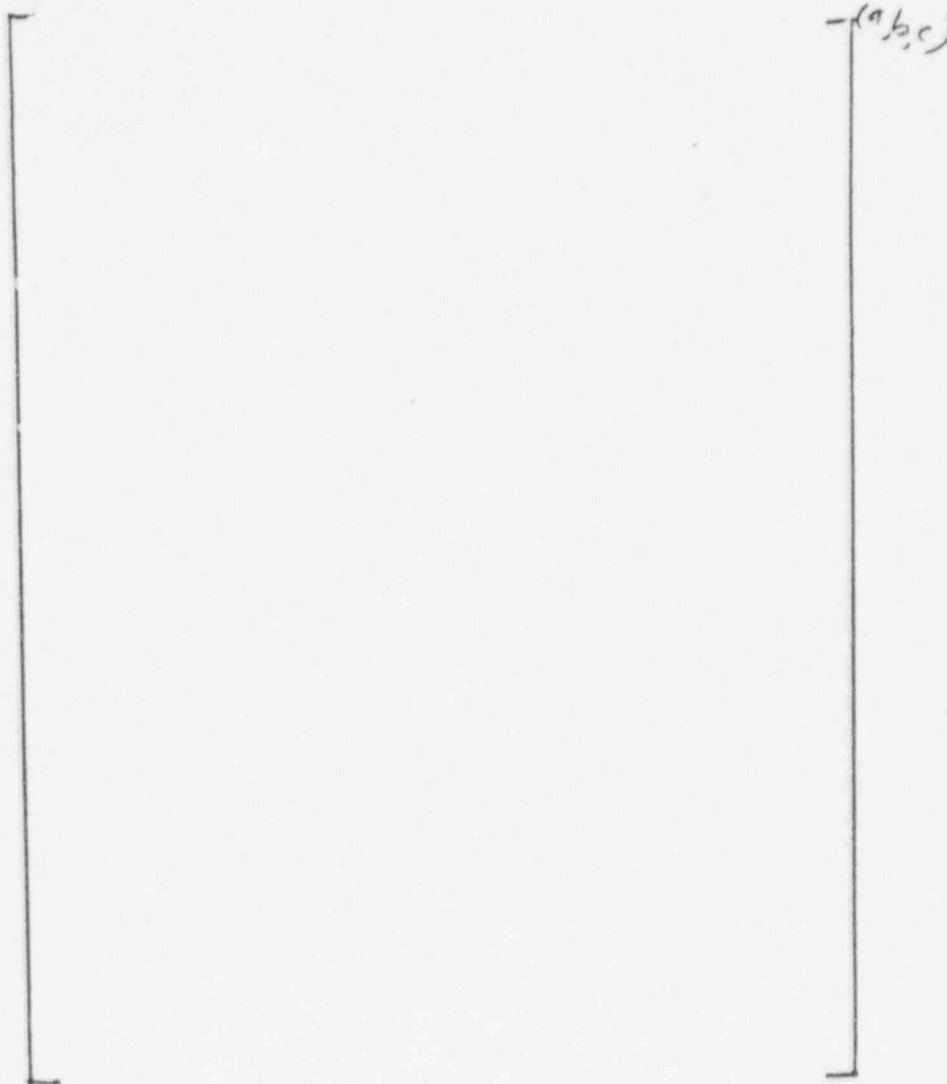
References

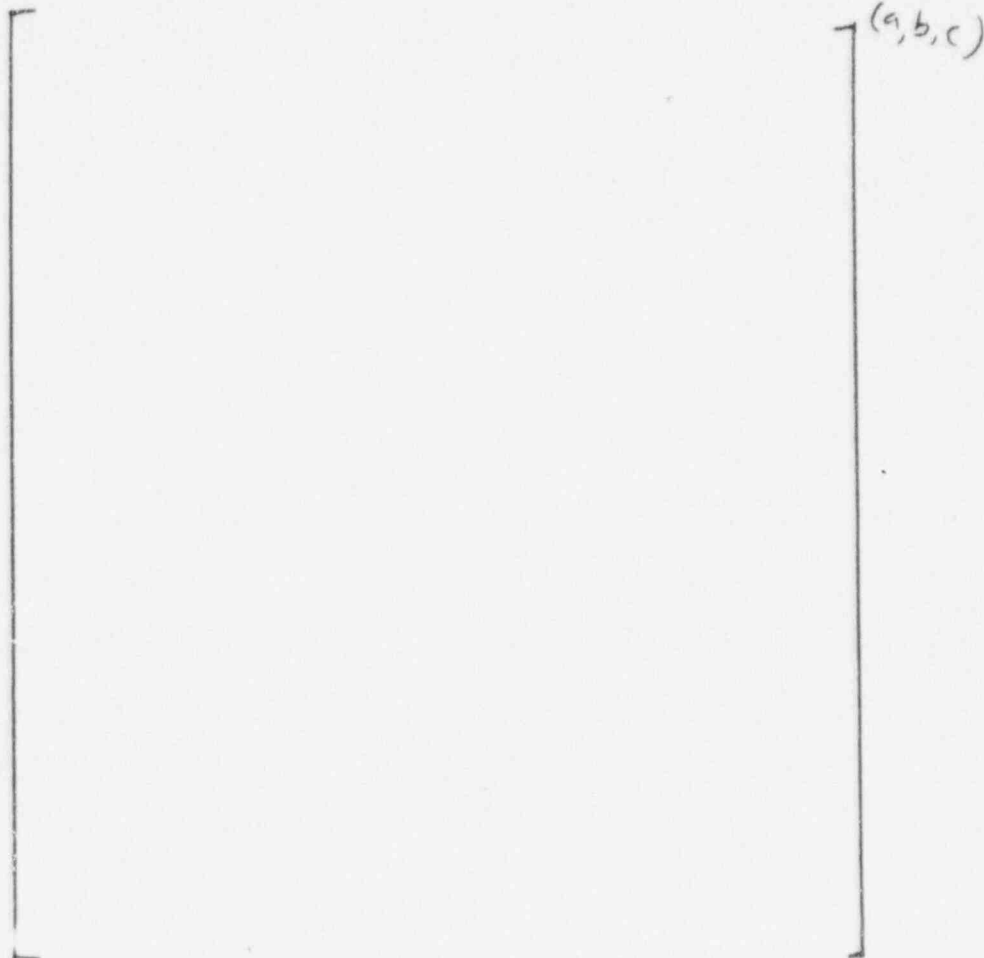
- 440.553-1 WCAP-14254, Revision 1, "AP600 SPES-2 Test Analysis Report," Proprietary [PXS-TZR-110], November 1995.

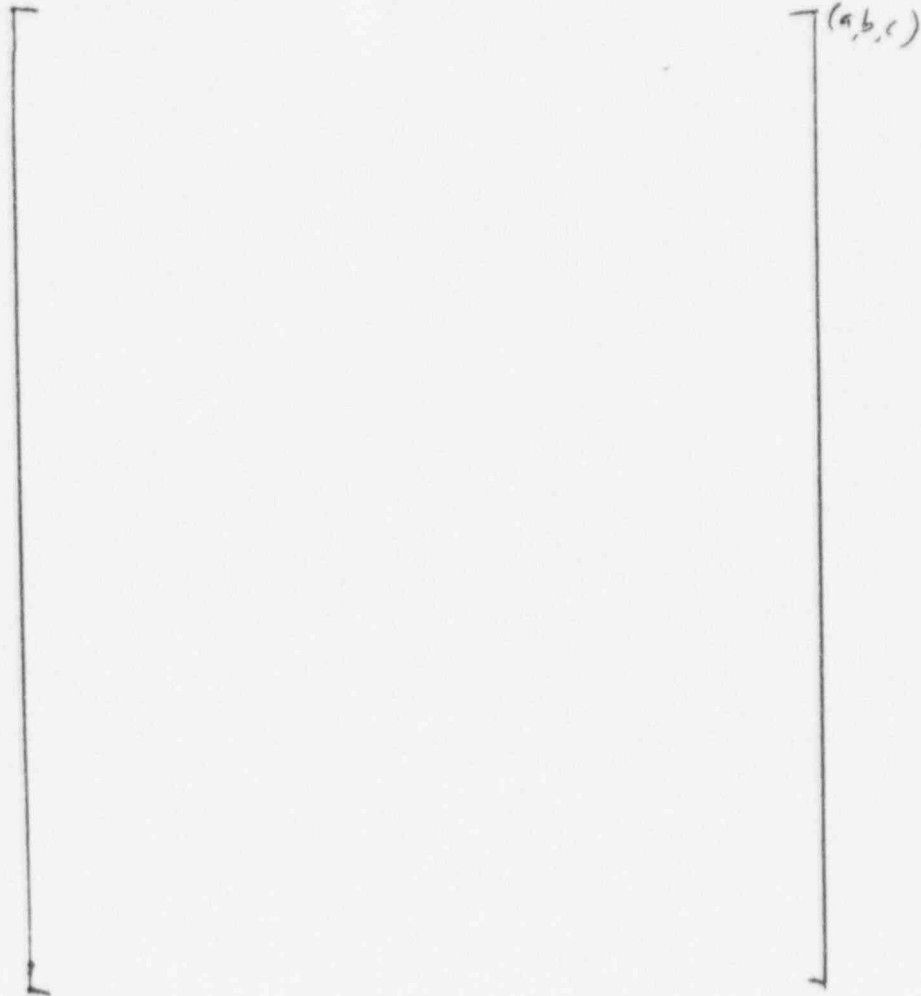
SSAR Revision: NONE

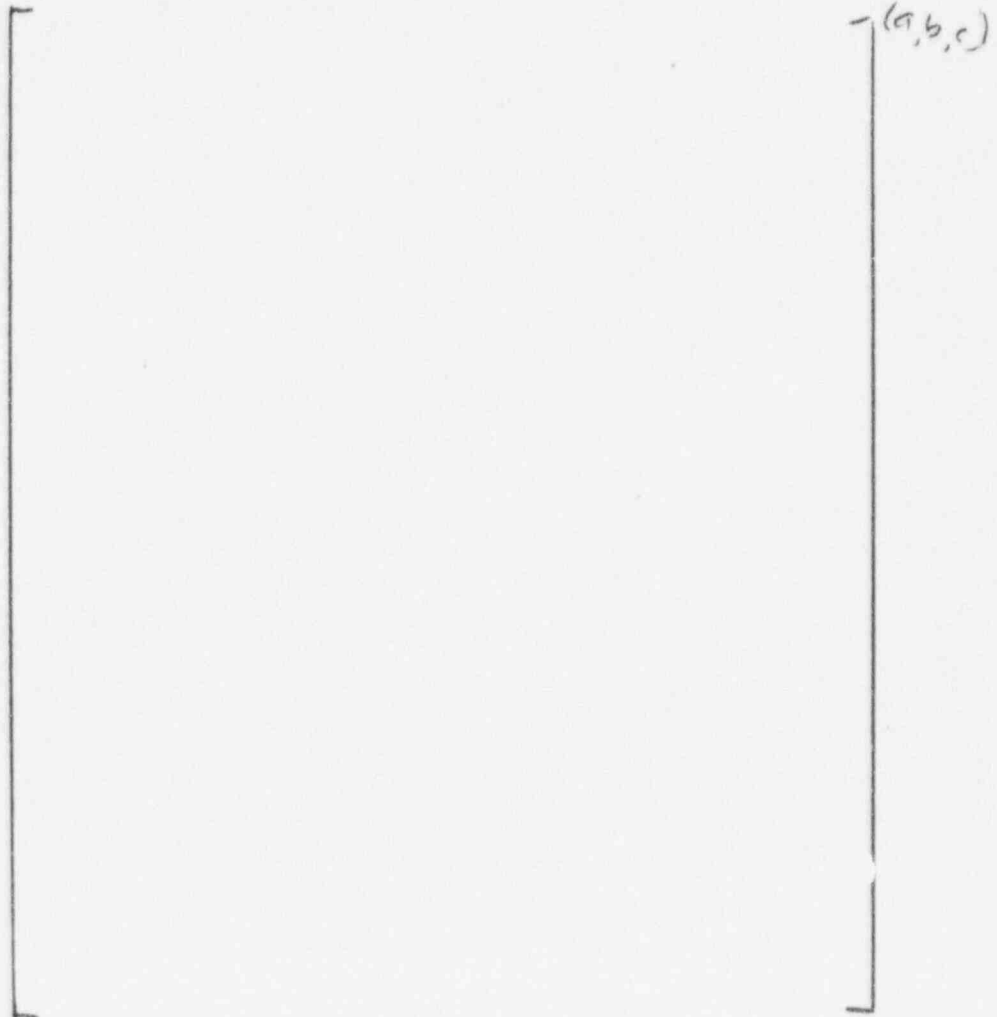


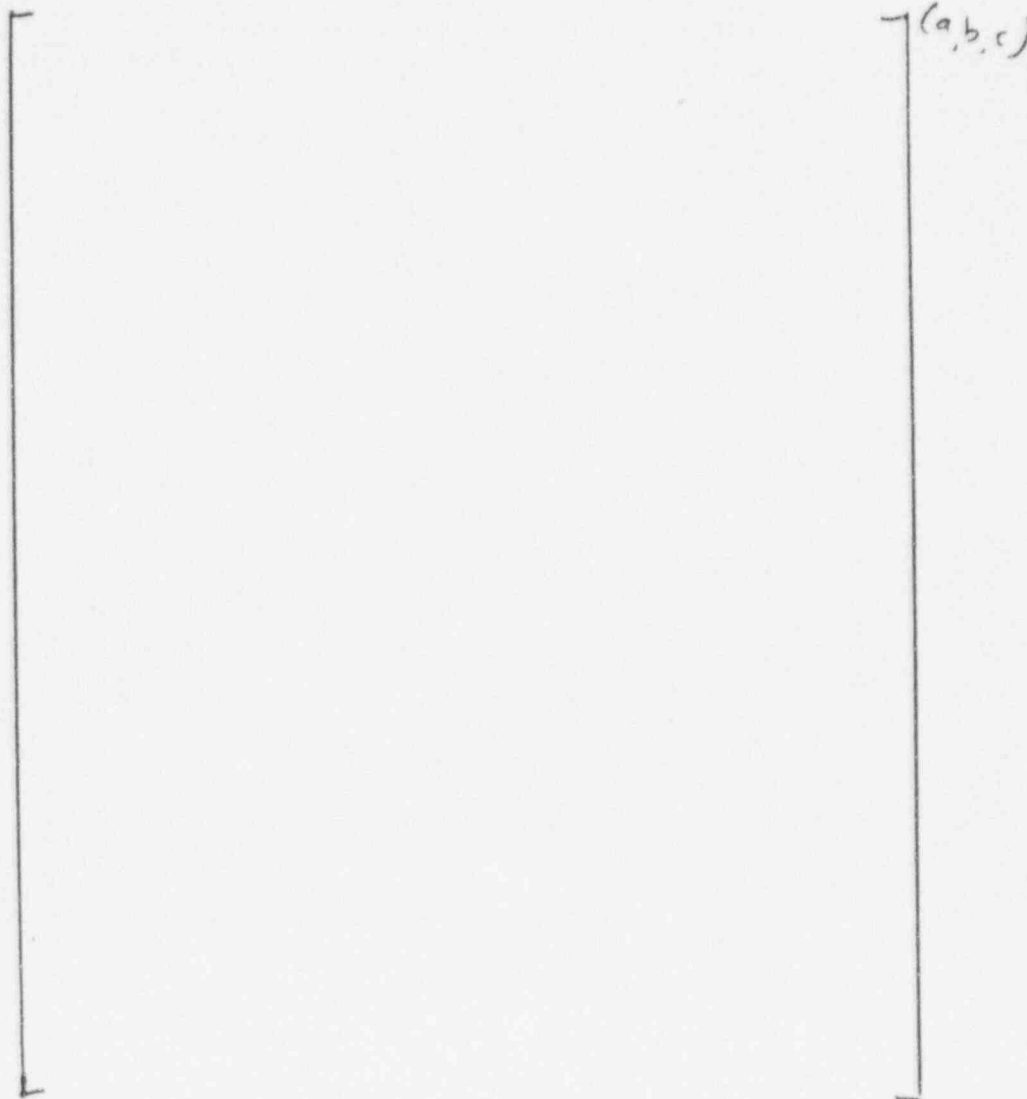
NRC REQUEST FOR ADDITIONAL INFORMATION

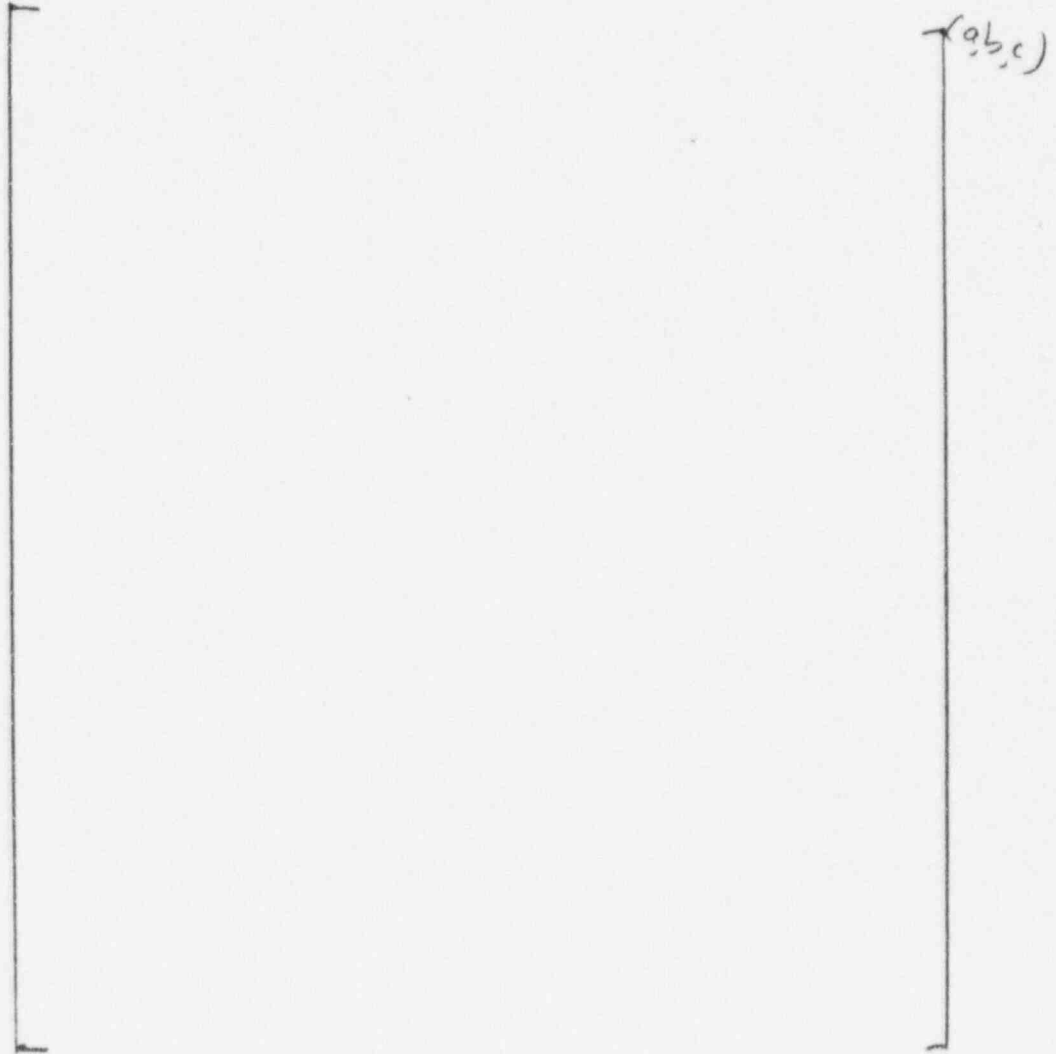


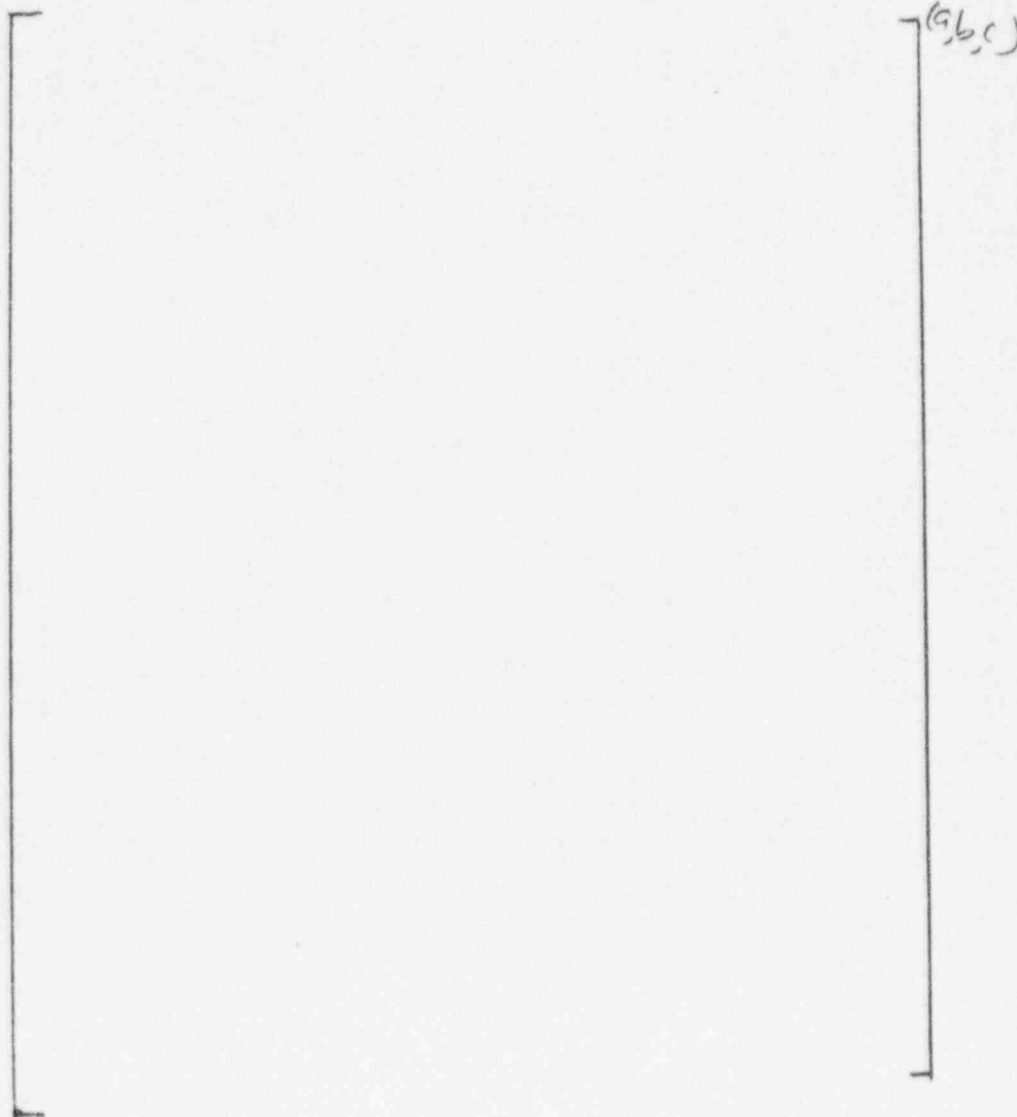


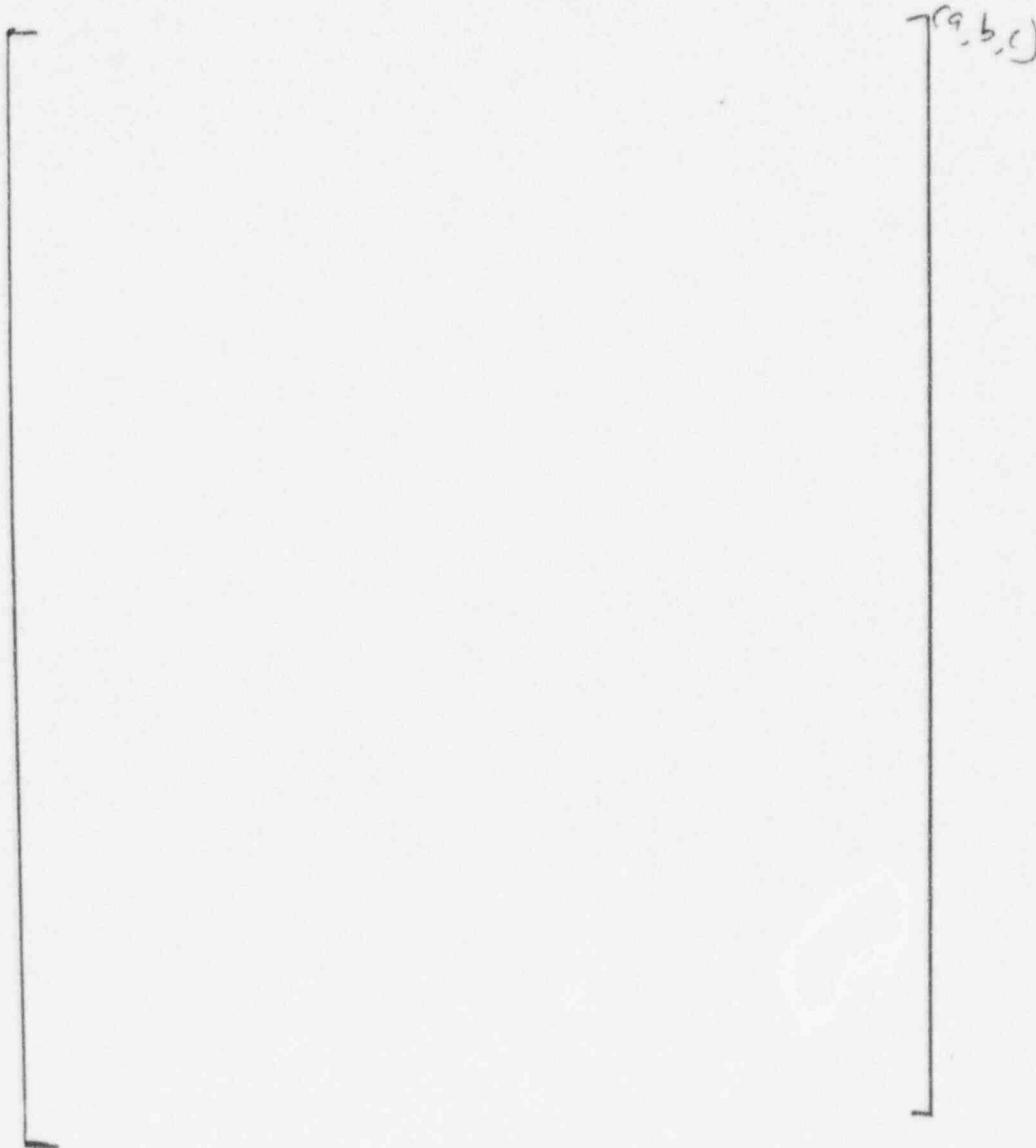


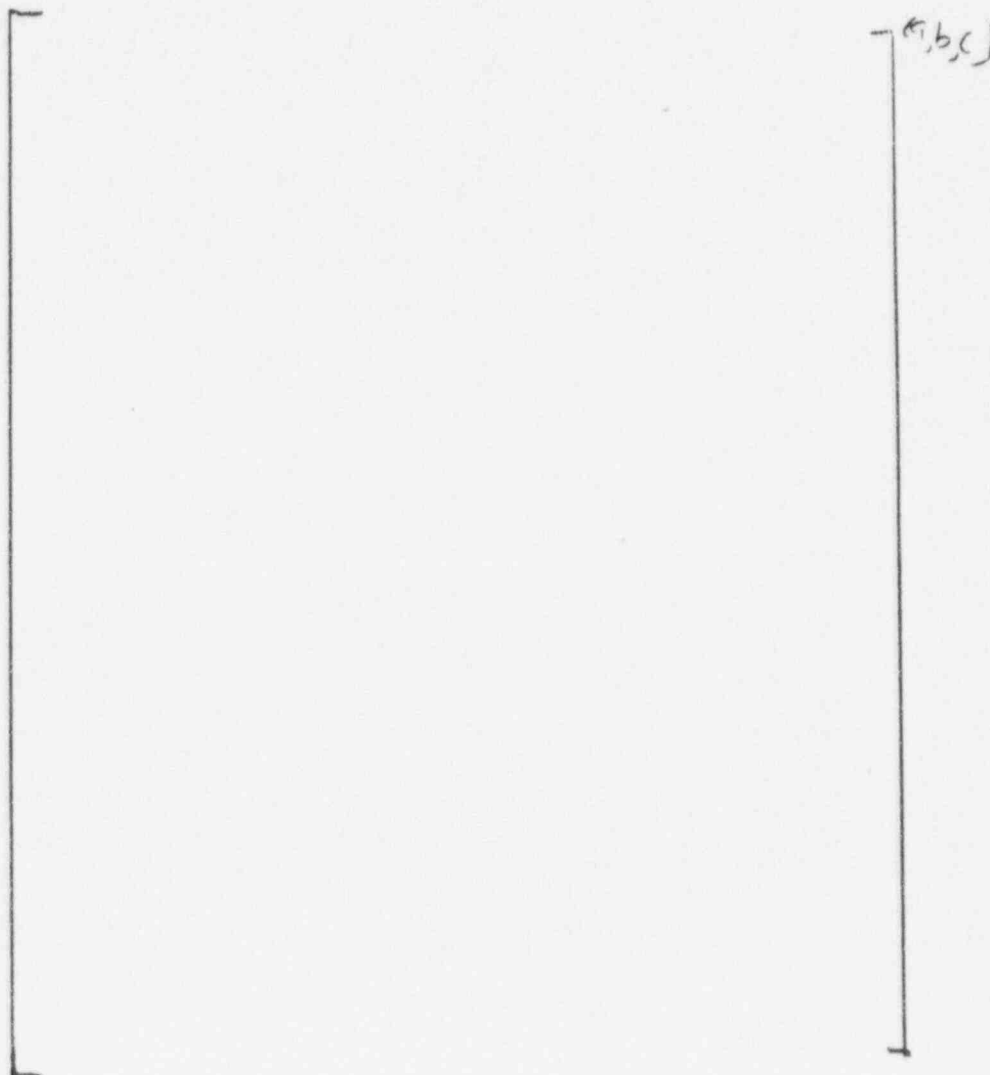












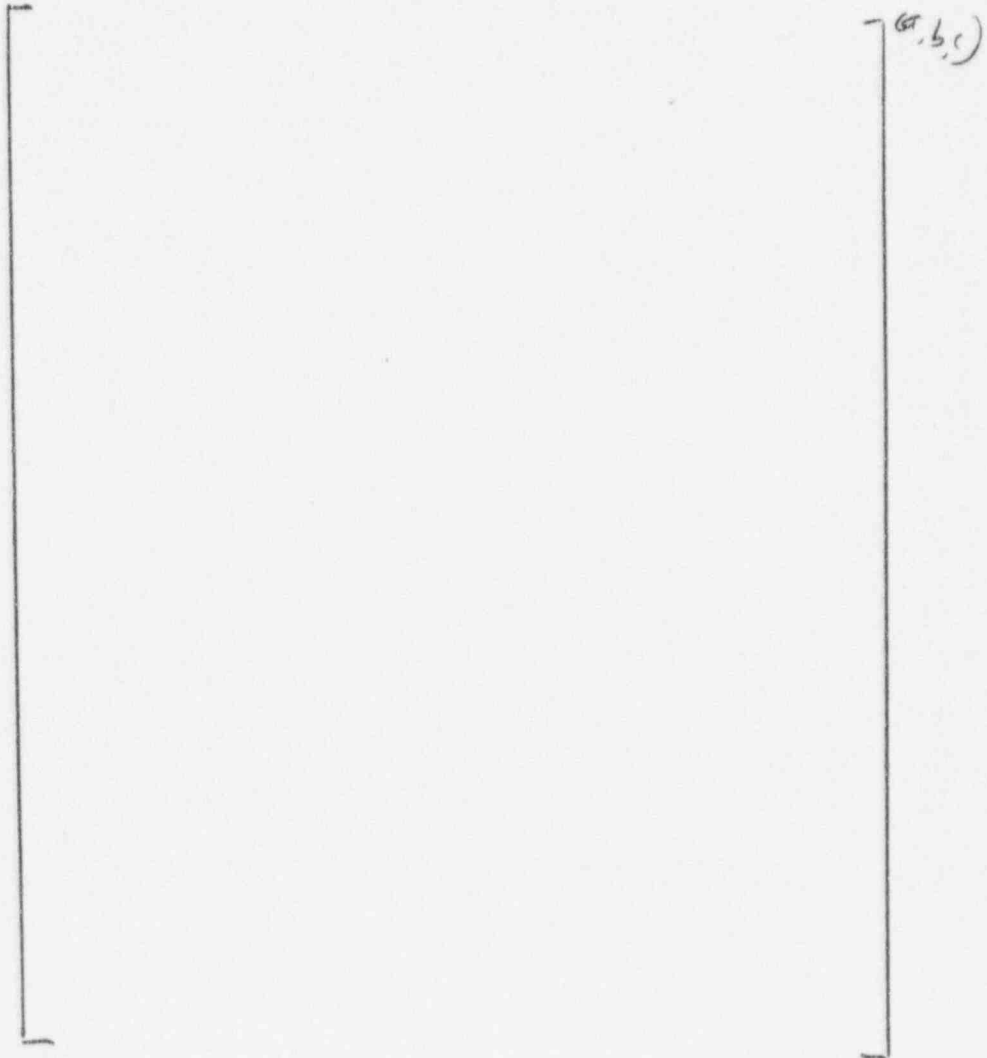


[

(a,b,c)

]



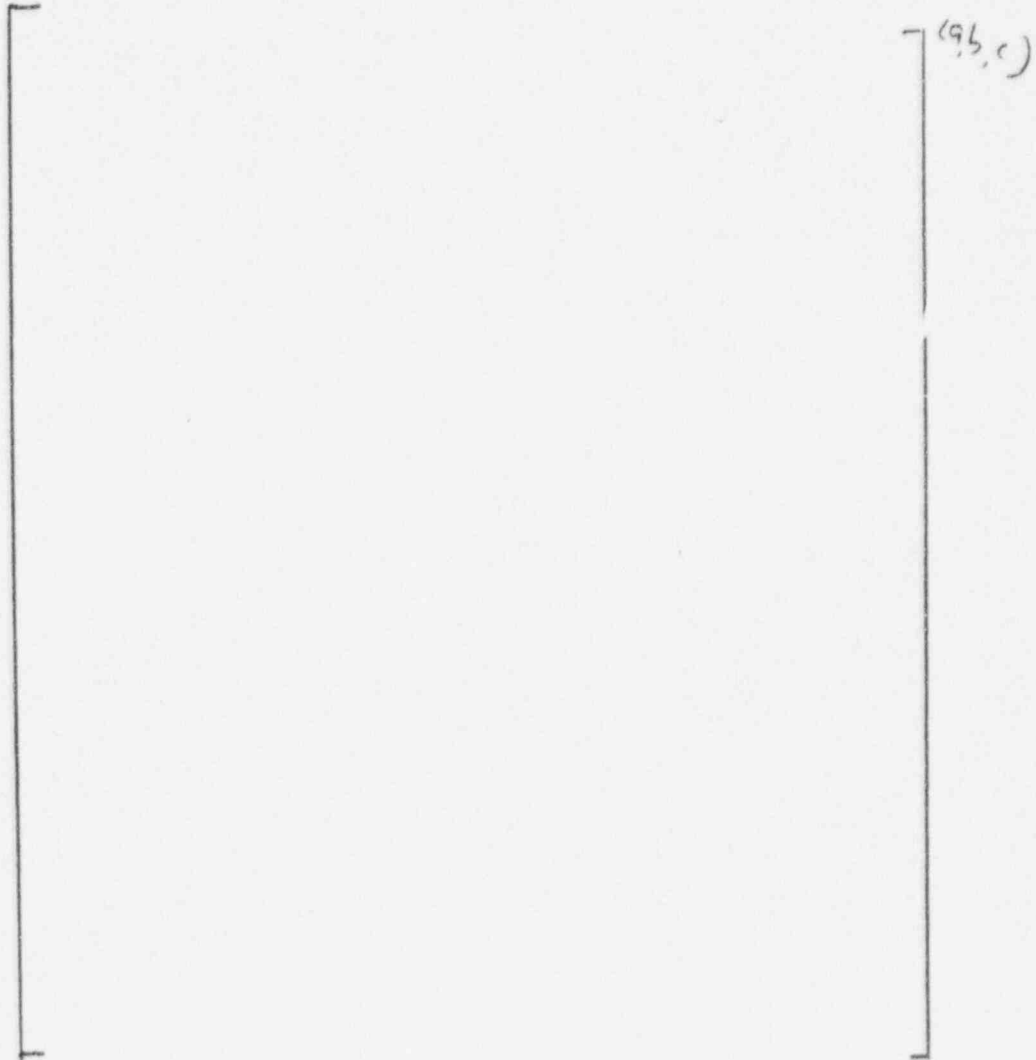


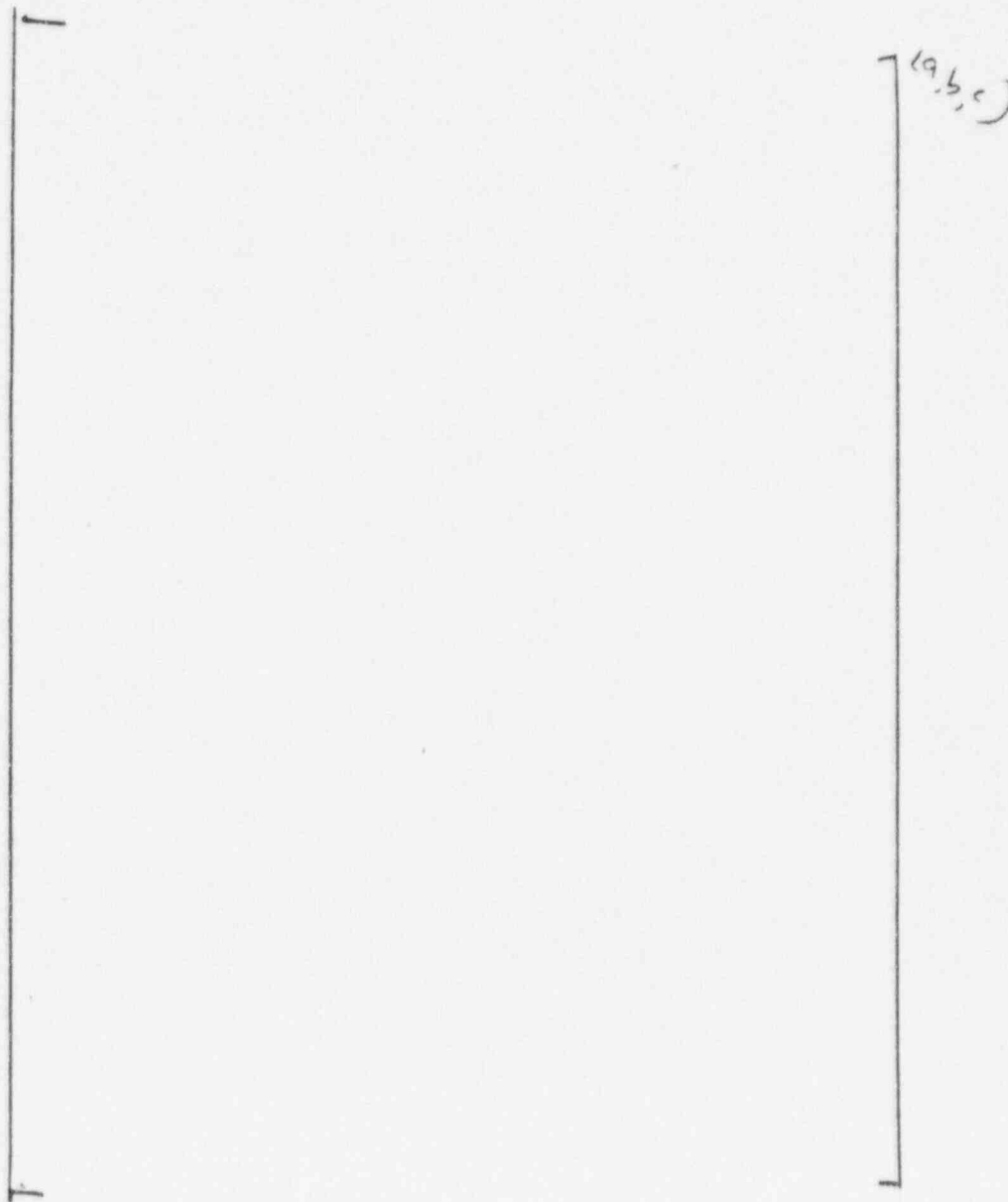


(a,b,c)











Question 480.242

Re: SPES-2, Test S01110

The results of this test show strong oscillatory behavior beginning at around 3000 seconds, as noted in the Summary. Westinghouse should be prepared to address this behavior in detail, especially the large oscillations in temperatures throughout the system (note, for instance, temperature oscillations of more than 100 F in cold leg temperatures on Plot 8). The mechanisms of the oscillations and their characteristics (e.g., which parameters are in-phase, and which are out-of-phase, and why) should be explained, as well as why this type of oscillatory behavior is (or is not) characteristic of what might be observed in the AP600 during a similar event. In addition, the oscillations appear to continue for more than an hour, with no signs of abating prior to termination of the test. If this system behavior is deemed to be possible in the AP600, Westinghouse should evaluate the period for which the oscillations would be expected to persist, and should also evaluate the impact on RCS components of oscillating temperatures, pressures, and liquid levels. Note that single steam generator tube ruptures have occurred in several plants in the operating fleet, and the staff considers such events more likely to occur than many of the other events evaluated for the AP600.

Response:

The mechanism for the oscillations observed in test S01110 (from approximately 3000 seconds to the end of the test) is the same as that described in Section 4.5.1 of Reference 480.242-1. At approximately []^{abc} into the transient, the upper plenum was completely drained to the hot leg elevation, and there is a general reduction in the natural circulation driven core flow. This flow decrease increases the core power to flow mismatch, so that a higher level of boiling commences. The increased rate of boiling results in a decrease in the density of the two-phase fluid on the hot side of the primary system. The pressure on the primary side of the steam generator U-tubes increases above that on the secondary side and much of the steam condenses so that the fluid on the cold side of the tubes is single phase. Since the driving head for the primary system natural circulation is the density difference between the two-phase fluid on the hot side of the primary circuit, and the single phase fluid on the cold side, there is a resultant increase in flow to the core. This produces a reduction in the level of core boiling, an increase in the hot side density and a subsequent decrease in core flow which enables the cycle to begin again.

Not all the steam entering the steam generator tubes is condensed, so there is a build-up of vapor at the top of the tubes. This build-up of vapor will reinforce the reduction in natural circulation flow. When this arises, it causes a further reduction in water level on the cold side of the tubes while the level on the hot side increases as water from the power channel enters the hot side tubes. Eventually the hot side tubes become full enough for water to once again flow to the cold side.

Unlike the LOCA cases, in the SGTR, there is no significant build-up of steam in the hot side steam generator tubes, and thus the tubes never fully drain. In the SGTR transient the natural circulation flow through the steam generator tubes is never fully stopped, and this explains why, once initiated, the oscillations continue to the end of the test in S01110, whereas they cease in the LOCA cases once the tubes drain.





Figures 480.242-1 to 480.242-6 illustrate this process for test S01110. It can be seen from Figures 480.242-1 and 480.242-2 that the variations in power channel pressure, saturation temperature and void fraction are all in phase. Figure 480.242-3 and 480.242-4 show that the void fraction variations in the steam generator tubes begin after those in the power channel, and they are almost exactly out of phase with those in the power channel. Figure 480.242-4 also shows how the response of the steam generator cold side tubes lags behind that of the hot side tubes, and that there is no prolonged build-up of steam on the hot side. The latter means the hot side tubes never fully drain and the oscillations thus continue to the end of the test. Figure 480.242-5 shows the response of the tubular downcomer flow to the steam generator cold side void fraction and Figure 480.242-6 shows how the core inlet flow drives the power channel void fraction variations.

For both test S01110 and the LOCA transients, the oscillations arise during periods when additional heat is being generated in the core to compensate for the higher heat losses expected in the SPES-2 facility relative to the AP600 plant. The LOFTTR analyses reported in Reference 480.242-2 did not show the oscillatory behavior. However, by the end of the LOFTRAN simulation ([]^{a,b,c}), the power channel has not fully drained to the hot leg elevation and thus the conditions necessary to initiate the oscillations have not arisen. Figures 480.242-7 to 480.242-8 compare results from the RELAP 5 MOD 3 V80 code analyses, described in Reference 480.242-1, undertaken to assess the response of the SPES-2 facility with heat loss compensation, compared to the expected AP600 response to a 2-inch LOCA. It can be seen that although the oscillations do occur in the AP600 predictions, they are of a lower amplitude than those observed in the SPES-2 predictions, because of the lower power in the core.

The SPES-2 tests, with the additional core power, demonstrate that there are large margins to core uncover, and that the oscillation mechanism is stable and well understood, it can therefore be concluded that the oscillations have no safety implication for the AP600 design.

References

- | | |
|-----------|-------------------------------------------------------------------------------------------------------------------------|
| 480.242-1 | WCAP-14254, Revision 1, "AP600 SPES-2 Tests Analysis Report," Proprietary [PXS-TZR-110], November 1995. |
| 480.242-2 | Final, "AP600 LOFTRAN-AP and LOFTTR2-AP Final Verification and Validation Report" Proprietary [PXS-GSR-100], June 1995. |

SSAR Revision: NONE





A large rectangular area enclosed by a thin black border, intended for providing additional information in response to the NRC request.







(b)(6)



Westinghouse

480.242-5





(b)(3)



Westinghouse

480.242-7



A large rectangular area enclosed by a thin black border, intended for providing additional information in response to the NRC request.





a, b, c

Figure 480.242-7



Figure 480.242-8

